The fitting of the hyperfine splitting of the $5 \rightarrow 4$ transitions in muonic Re-185

Stella Vogiatzi

ETH Zürich
Paul Scherrer Institut (PSI)

vstella@student.ethz.ch

October 2, 2018

My work

Part A:

Measurement of the efficiency of the veto detectors used in muX

Part B:

Development of the fitting procedure of the $5g \rightarrow 4f$, $5f \rightarrow 4d$ hyperfine transitions in Re-185

Introduction

muX project aims to measure the nuclear charge radius of ^{226}Ra with a precision of 0.2 %
$\rightarrow$ to be used in the atomic parity violation experiment with one single trapped ion Ra^{+}

Ways to measure the nuclear charge radii:

- optical and K X-rays isotope shifts $\rightarrow$ differences of RMS nuclear charge radii between different isotopes

- electron scattering
- muonic atom X-rays spectroscopy

$\rightarrow$ absolute values of RMS nuclear charge radii

Muonic atom

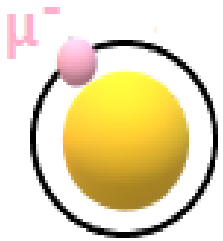

Muonic atom

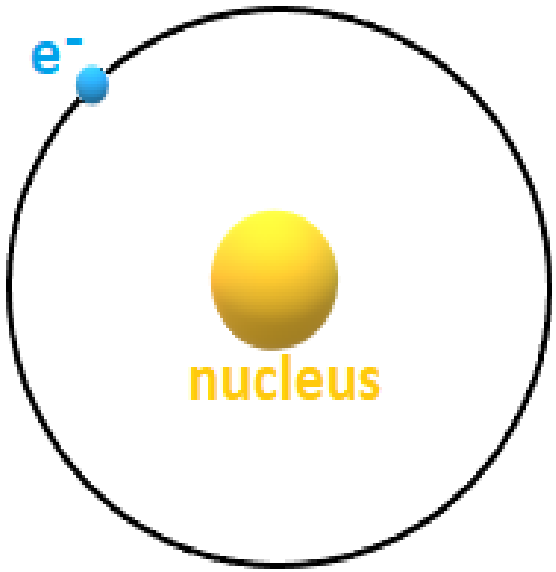

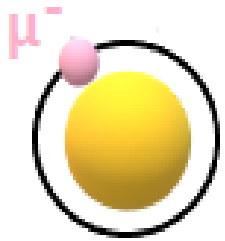

At Bohr approximation:

$$\left.\begin{array}{l} E_n \cong -m_\ell c^2 \frac{(\alpha Z)^2}{2n^2} \\ r_n \cong \frac{n^2}{m_\ell c^2} \frac{\hbar c}{\alpha Z} \\ m_\mu \simeq 206.8 m_e \end{array}\right\} \xrightarrow{n_{e-} = n_{\mu-}} r_{\mu-} \cong \frac{r_{e-}}{206.8}\,, \quad E_{\mu-} \cong 206.8\, E_{e-}$$

Muonic atom spectroscopy

1. Atomic capture (direct)
   - slow down in momentum
   - capture by the Coulomb field of nucleus

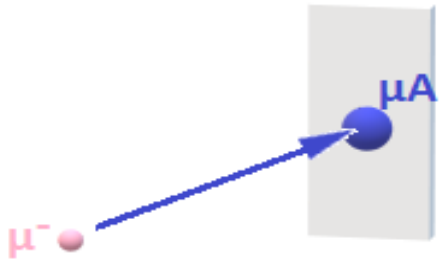

1. Muonic cascade to the ground state (1s)

2. Muon decay
   - free muon decay ($\tau \simeq 2.2\,\mu s$): $\mu^- \rightarrow e^- + \overline{\nu}_e + \nu_\mu$
   - muon nuclear capture ($\tau \simeq 80\,ns$): $\mu^- + (N, Z) \rightarrow (N+1, Z-1)^* + \nu_\mu$

Muonic atom spectroscopy - Muonic cascade

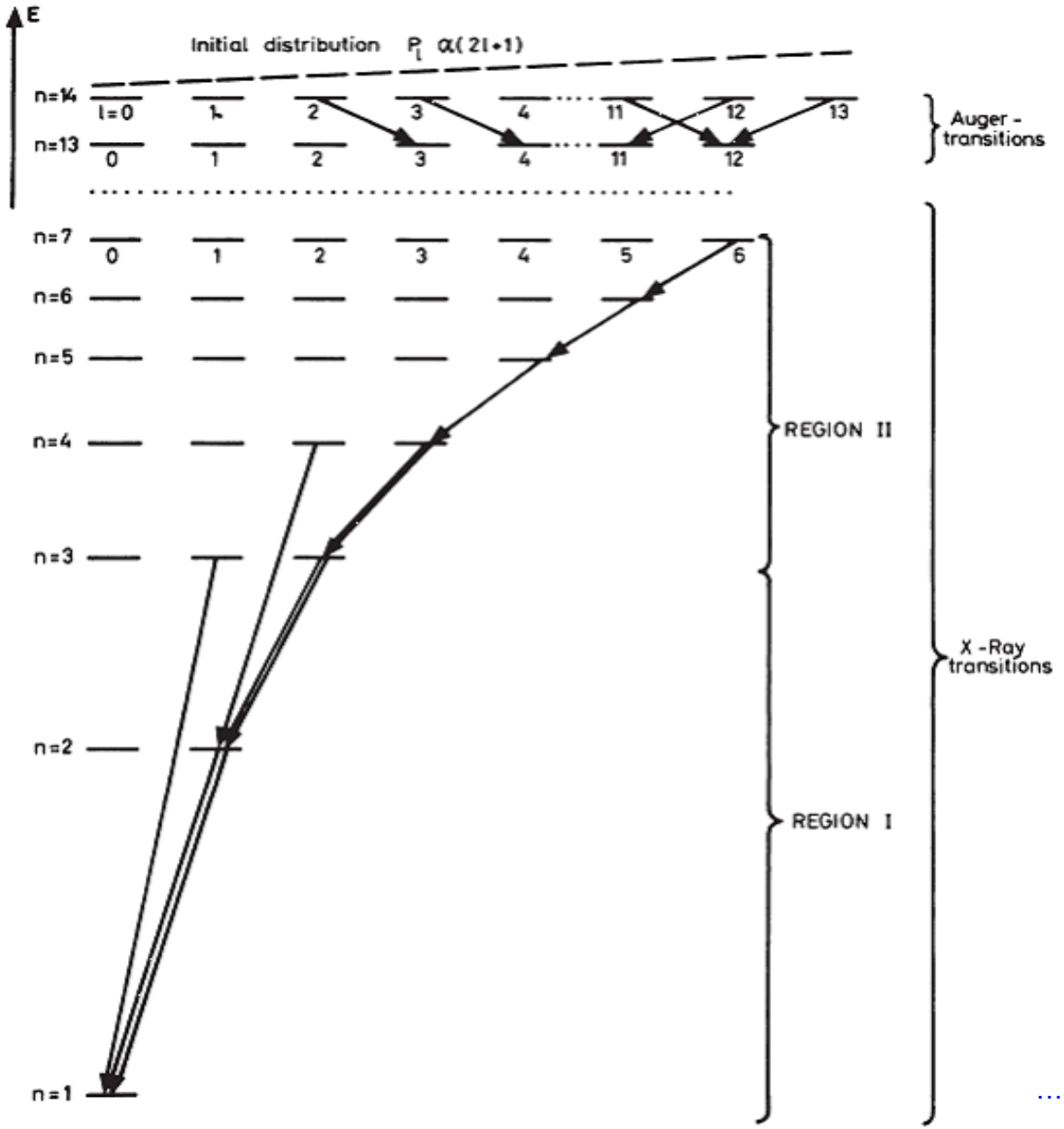

- Cascade starts at high n
  - ✓ For $n \gtrsim 6 \rightarrow$ Auger emissions
  - ✓ For $n \lesssim 6 \rightarrow$ X-rays
- $n_{\mu^-} = 14$ is below the $n_{e^-} = 1$ (K-shell)
- statistical distribution $P_l \sim (2l+1)$: $(n, l = n-1) \rightarrow (n-1, l = n-2)$ most intense transitions.

...at 1s state muon is captured by nucleus or decays

Muonic atom spectroscopy

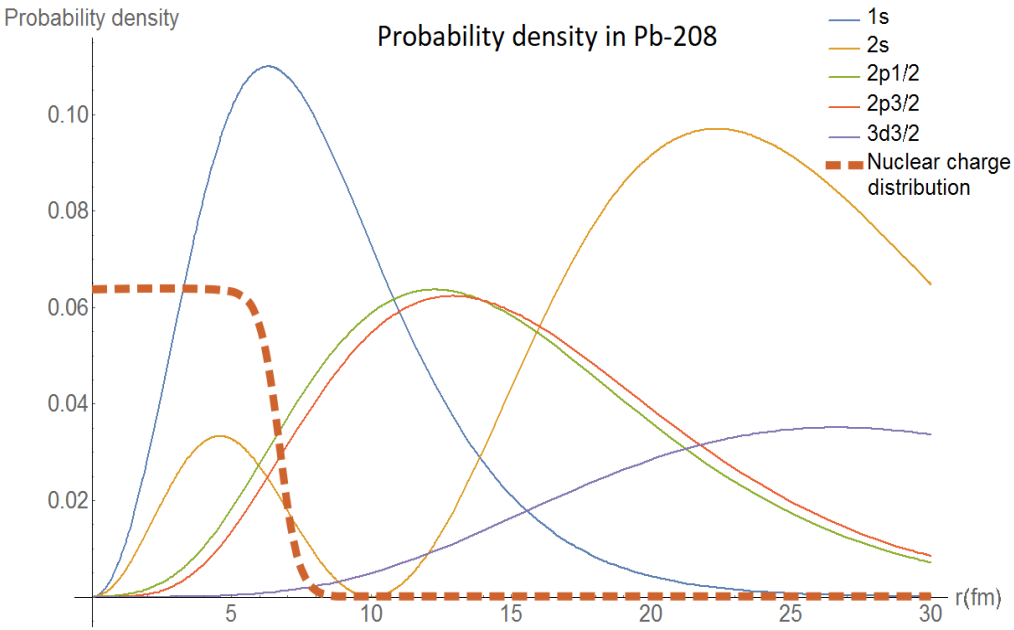

- Large overlap of the **low-lying states** with the nuclear charge distribution
- After $n \cong 6$, finite size effect is negligible

Two-parameter Fermi nuclear charge distribution:

$$\rho(r) = \frac{1}{1 + e^{\frac{r-c}{\alpha}}}$$

state	$(E_B^0 - E_B^{FS})/E_B^0$
$1s_{1/2}$	45.50 %
$2p_{1/2}$	8.16 %
$2p_{3/2}$	3.52 %
$4d_{3/2}$	0.11 %
$4d_{5/2}$	0.044 %
$5f_{5/2}$	0.0005 %
$6h_{9/2}$	< 0.0005 %

Apparatus during beam time 2016

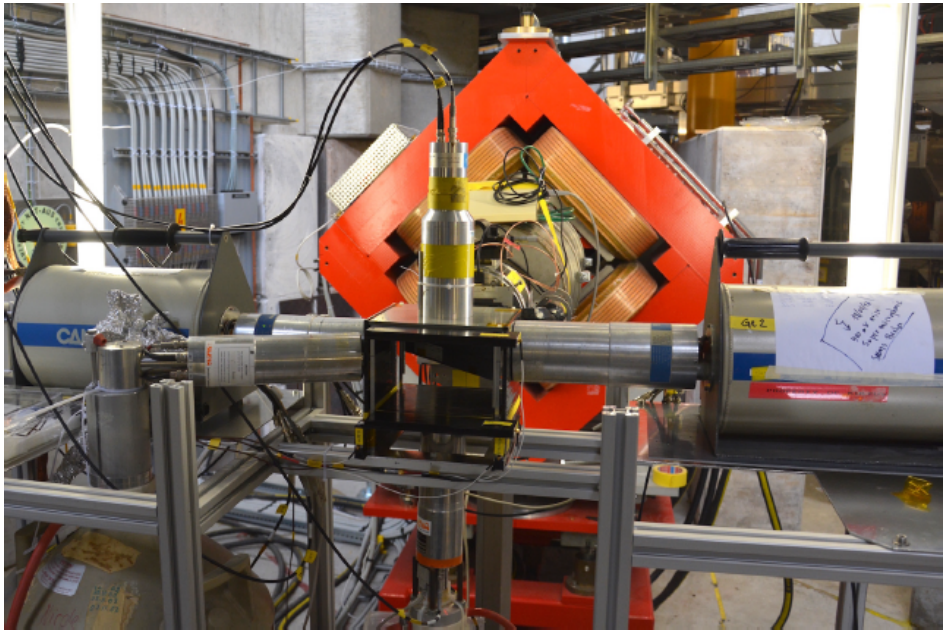

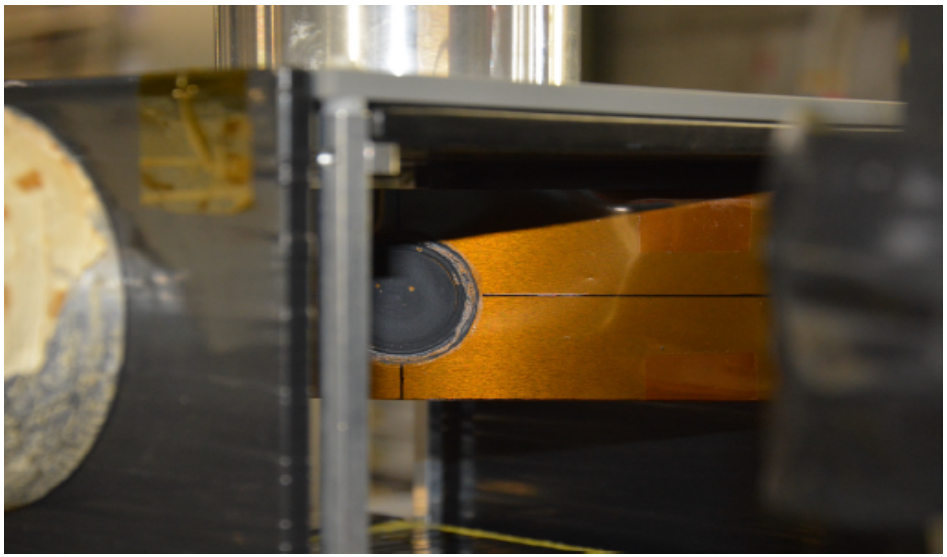

- Four HPGe detectors, only two operating properly working:

  Relative efficiency:
  - 20 % (GeR)
  - 75 % (GeL)

  Energy resolution at 1332.5 keV:
  - 0.92 keV (GeR)
  - 1.23 keV (GeL)
- one brillance detector
- six plastic scintillators:
  - muon veto
  - muon entrance
  - four veto detectors
- target:
  500 mg Re-185, Re-187
  1000 mg Pb-208

Estimation of the absolute efficiency of the veto detectors

Veto detectors to be tested

- BC-400 organic scintillator
- coupled to SiPM detectors

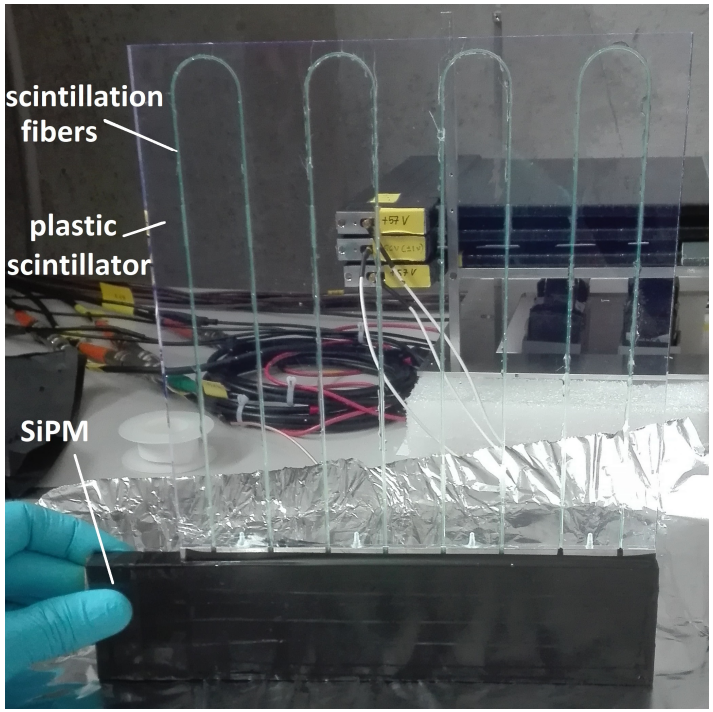

- 7 veto detectors:
  5 Sc of $180 \times 180\,\mathrm{mm}^2$, 5 mm thick
  2 Sc of $180 \times 150\,\mathrm{mm}^2$, 5 mm thick
- Presence of hole at the center of 3 veto detectors (used in measurement with gas cell):
  $d \cong 35\,\mathrm{mm}$ (in 2 Sc)
  $d \cong 22\,\mathrm{mm}$ (in 1 Sc)

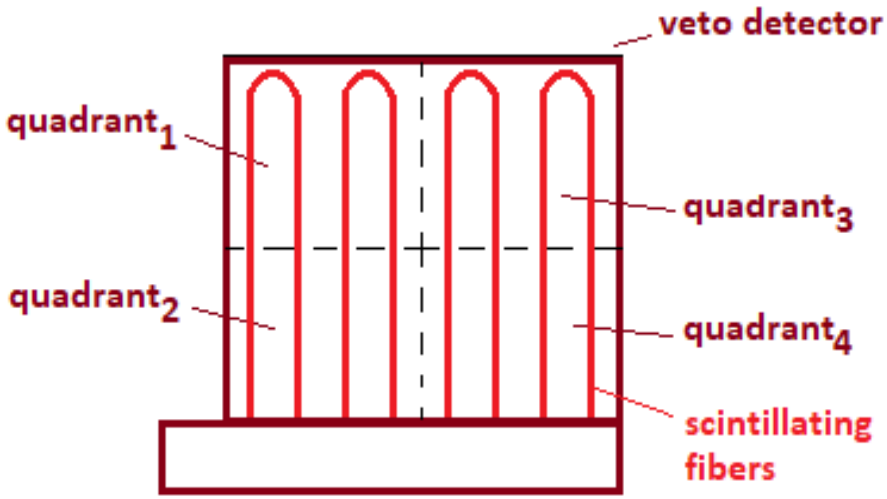

Measurement apparatus with **cosmic rays**

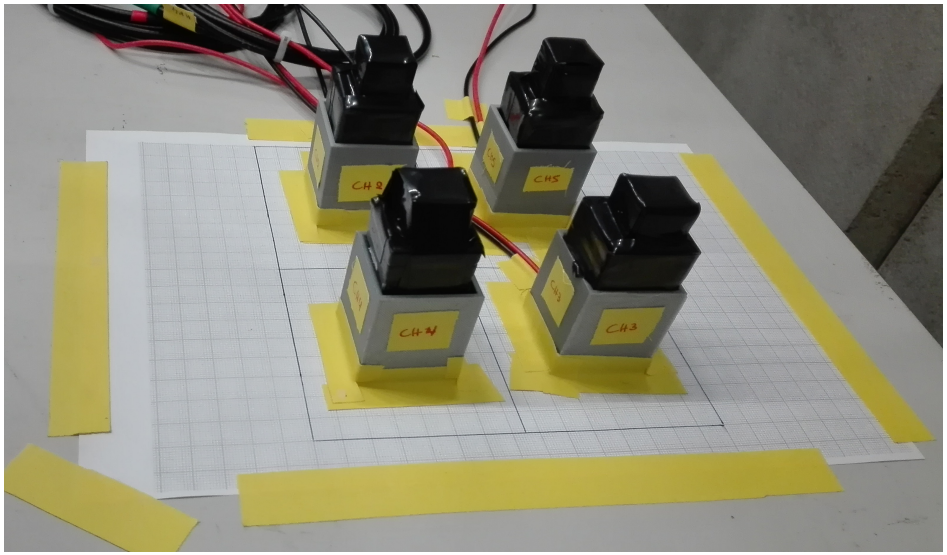

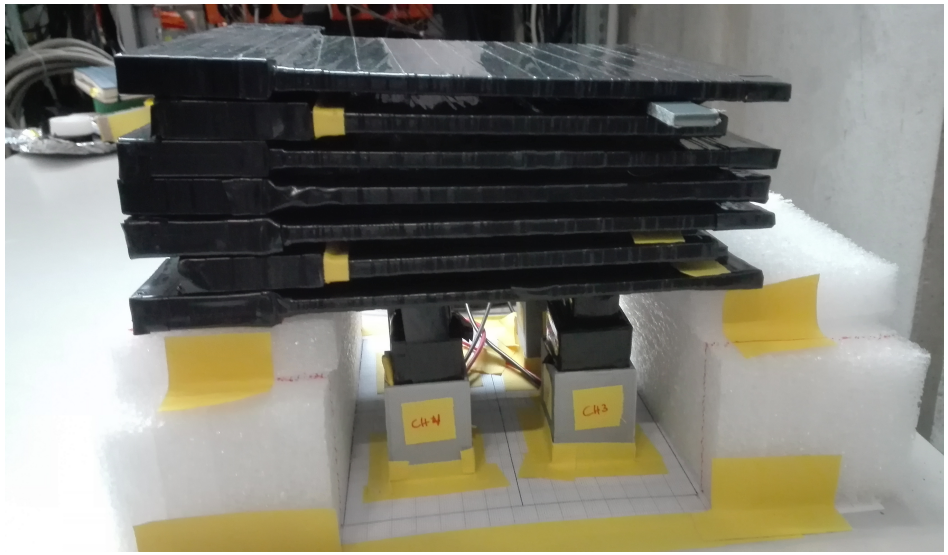

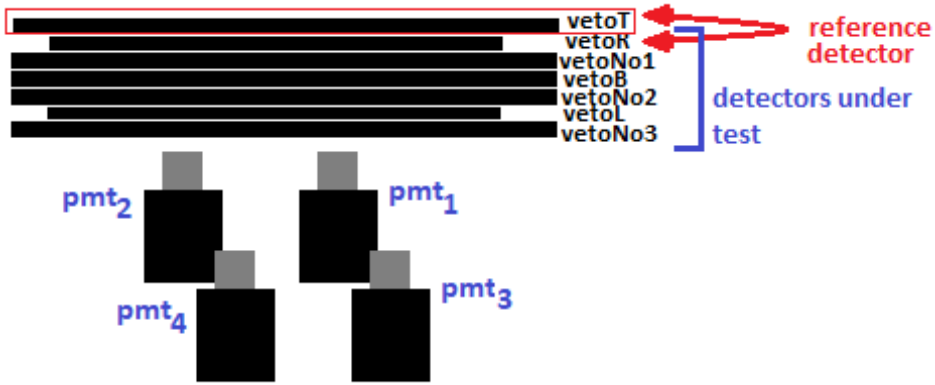

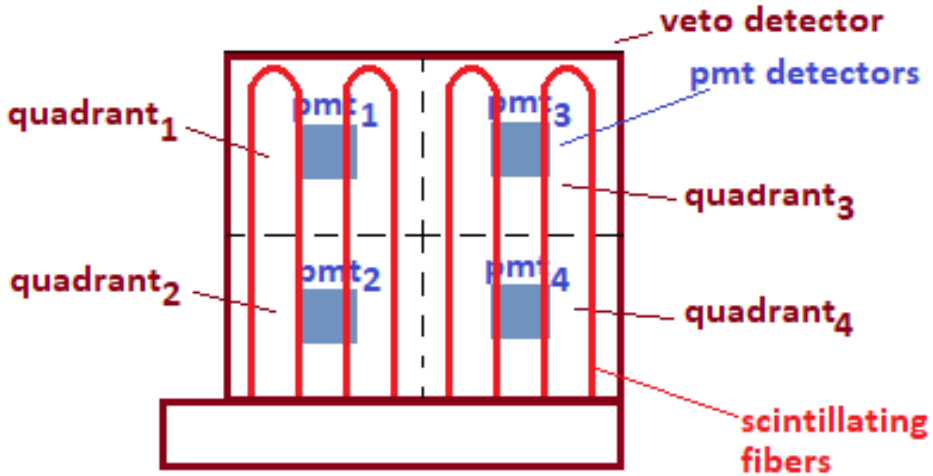

Single energy spectra

Energy spectra (85 hours of data acquisition)

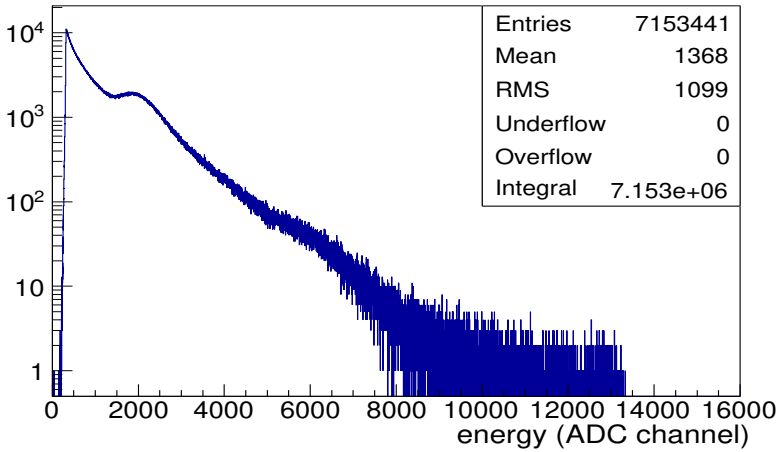

veto detector ($veto_T$)

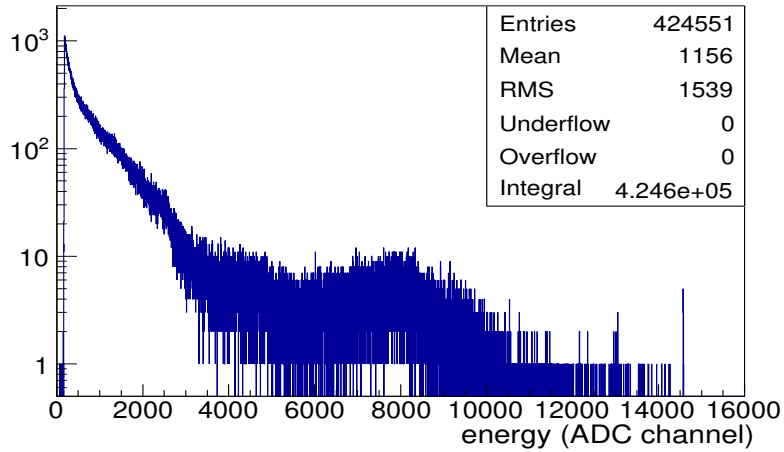

pmt detector (pmt_1)

Time difference distribution

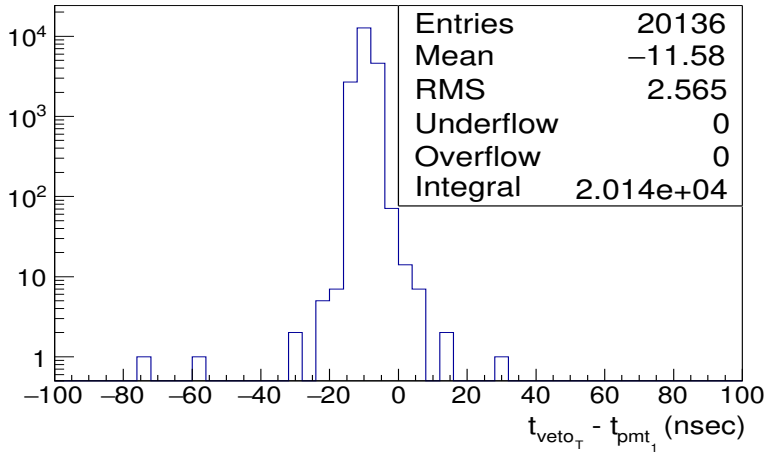

PMT coincidence energy spectra

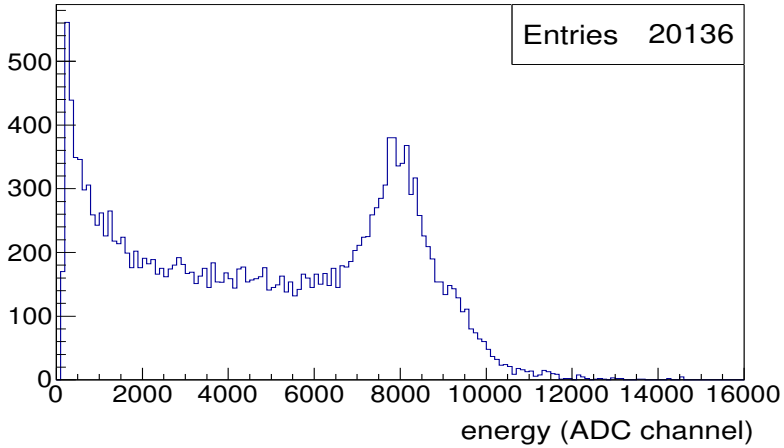

pmt_1

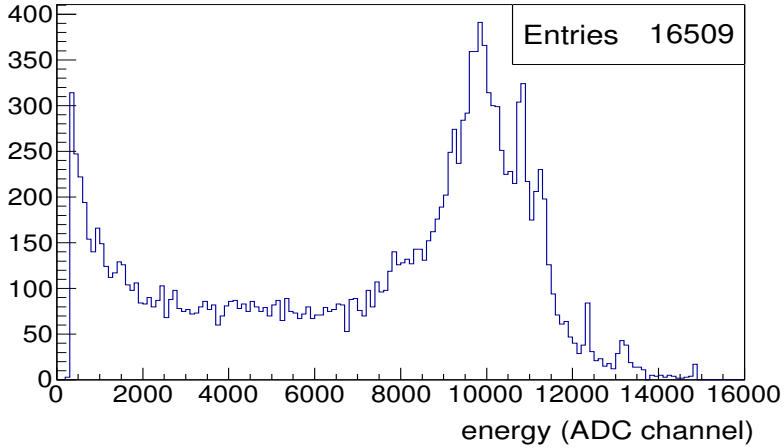

pmt_2

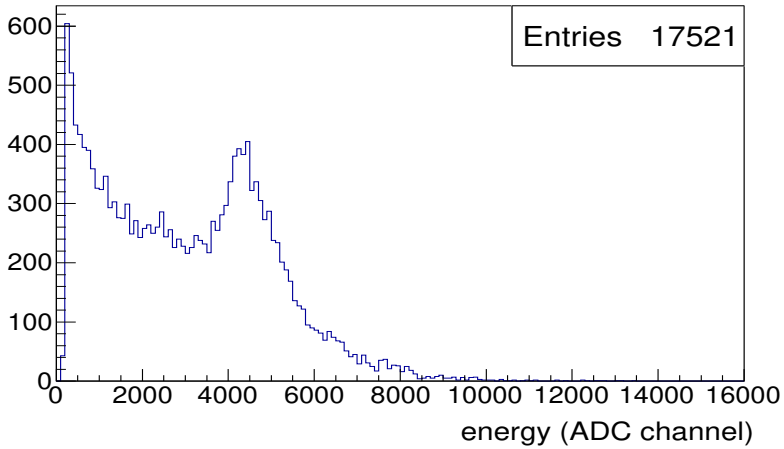

pmt_3

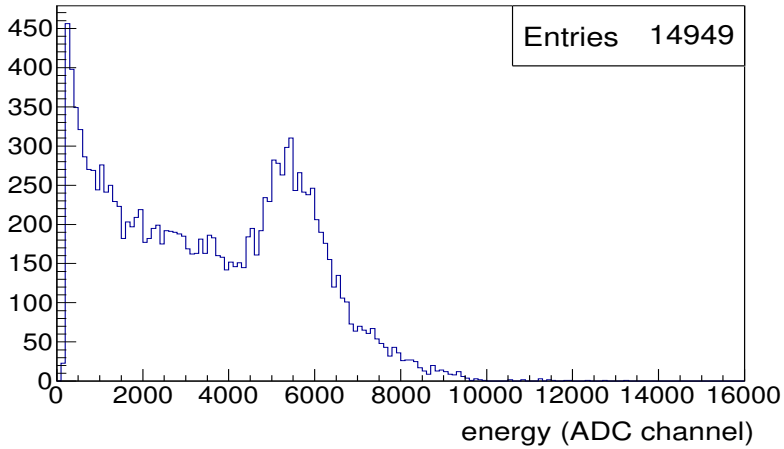

pmt_4

PMT coincidence energy spectra

Selection of straight cosmic rays

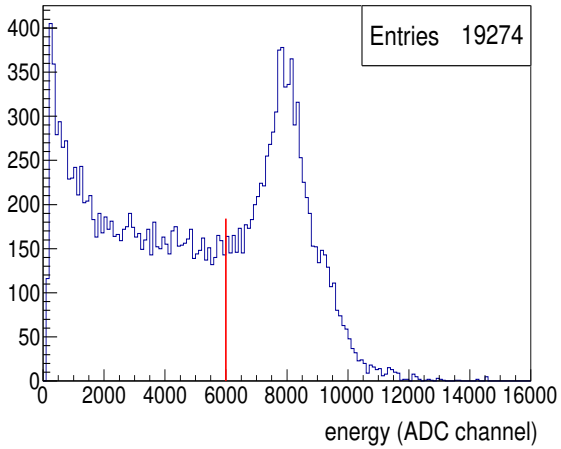

pmt_1

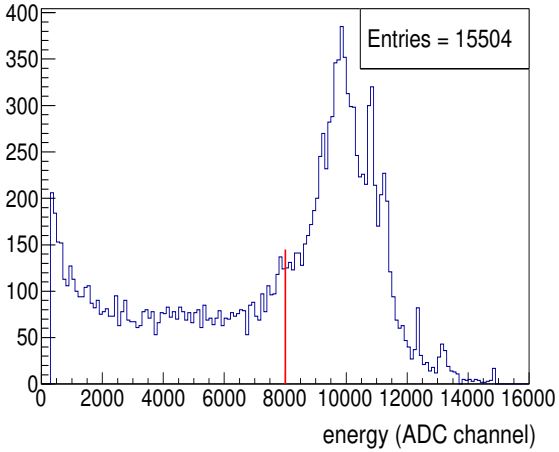

pmt_2

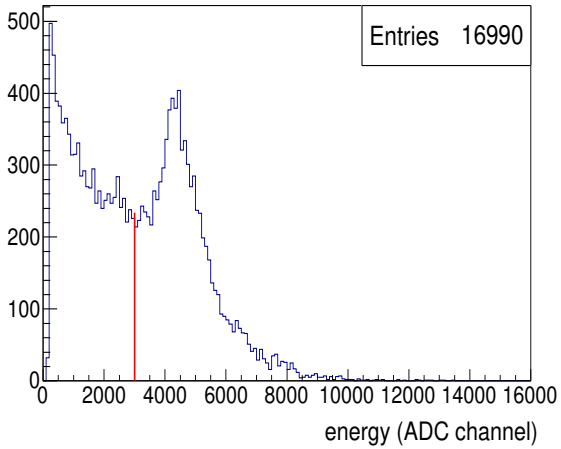

pmt_3

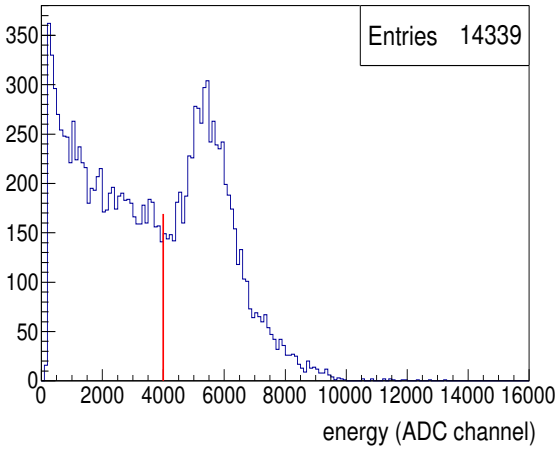

pmt_4

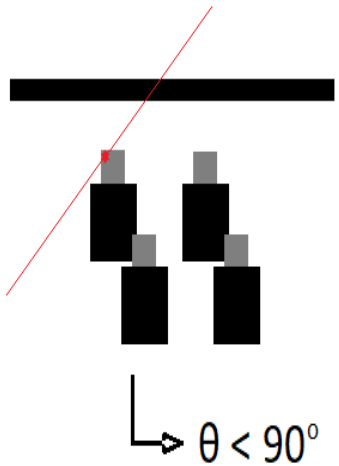

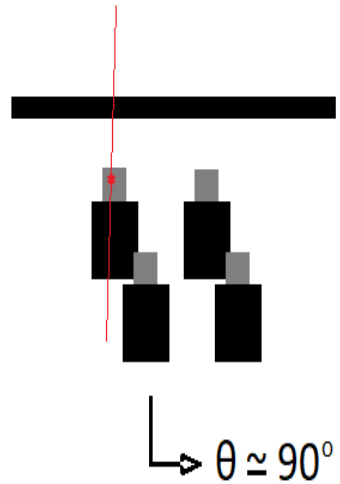

Veto coincidence energy spectra

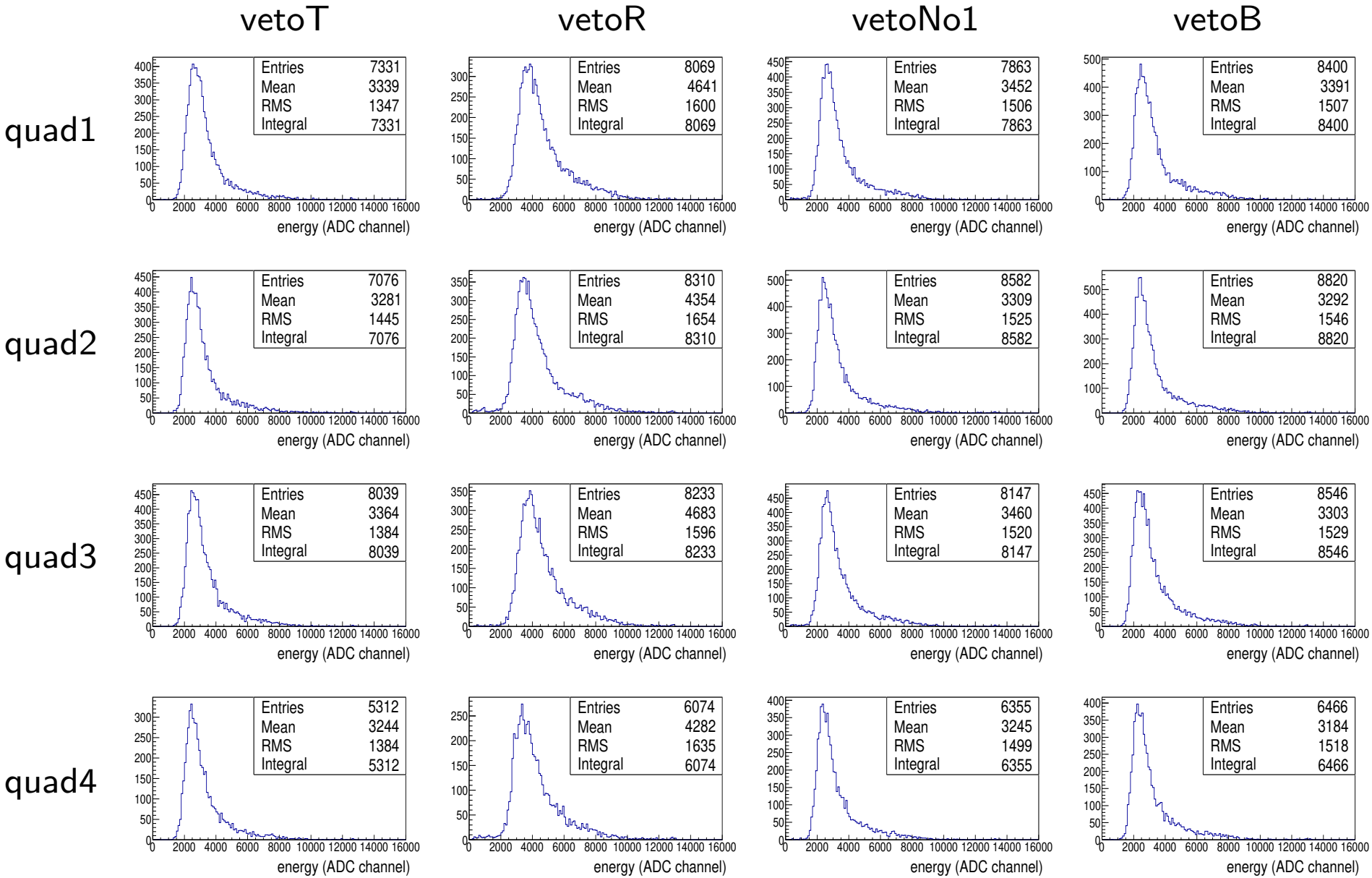

Veto coincidence energy spectra

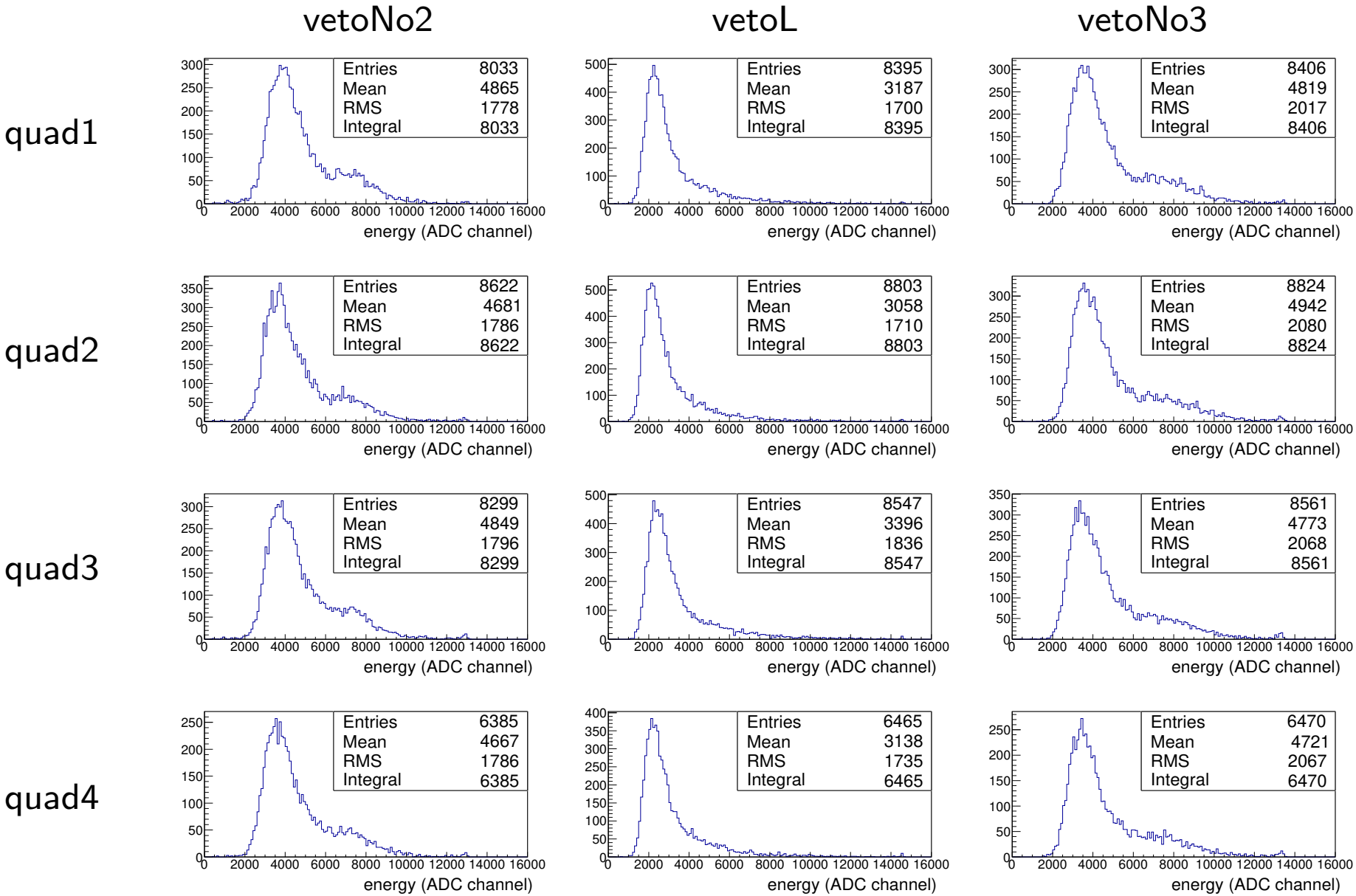

Absolute efficiency combined results

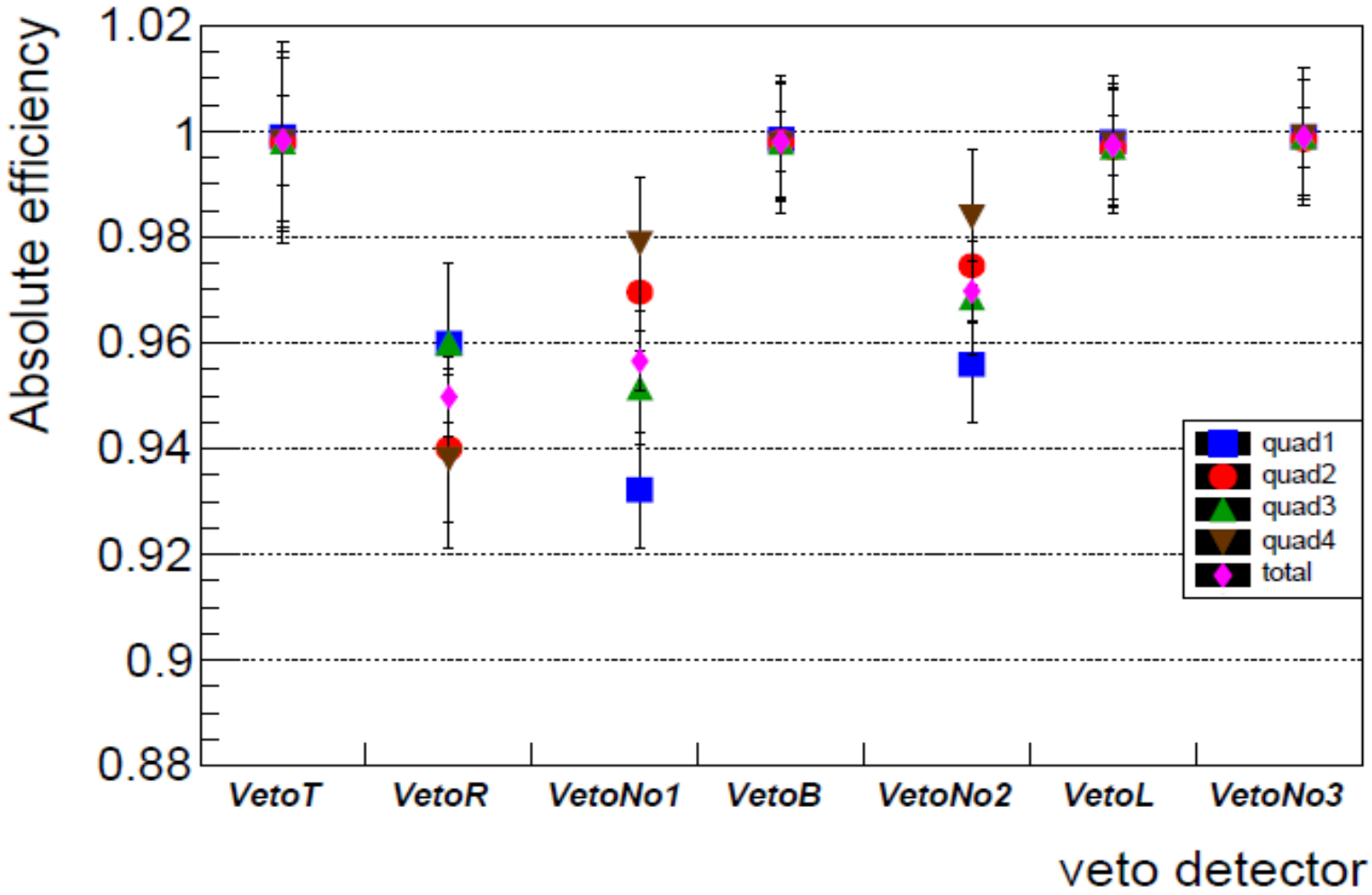

Fitting of the 5g-4f and 5f-4d hyperfine transitions in Re-185

Energy levels in μRe-185

Re-185 is:

- ✓ stable element
- ✓ nuclear charge radius has not been measured yet
- ✓ nuclear spin at ground level $I = 5/2 \rightarrow$ HF effect in the energy splitting levels $(\vec{F} = \vec{I} + \vec{J})$

- Energy displacement due to the electric quadrupole interaction:

$$\Delta E_F\,(E2) = A_2\, 6\, \frac{K(K+1) - 4/3\, I(I+1)J(J+1)}{4I(2I-1)J(2J-1)}$$

where $K = F(F+1) - I(I+1) - J(J+1)$.

- Energy displacement due to the magnetic dipole interaction:

$$\Delta E_F(M1) = \frac{A_1}{2}\,\{F(F+1) - I(I+1) - J(J+1)\}$$

A_2 : E2 hf constant $\rightarrow Q$ dependence

A_1 : M1 hf constant $\rightarrow \mu_N$ dependence

far away from the nucleus
total Q, μ_N

$5g_{9/2} \rightarrow 4f_{7/2}$ hyperfine transition in Re-185

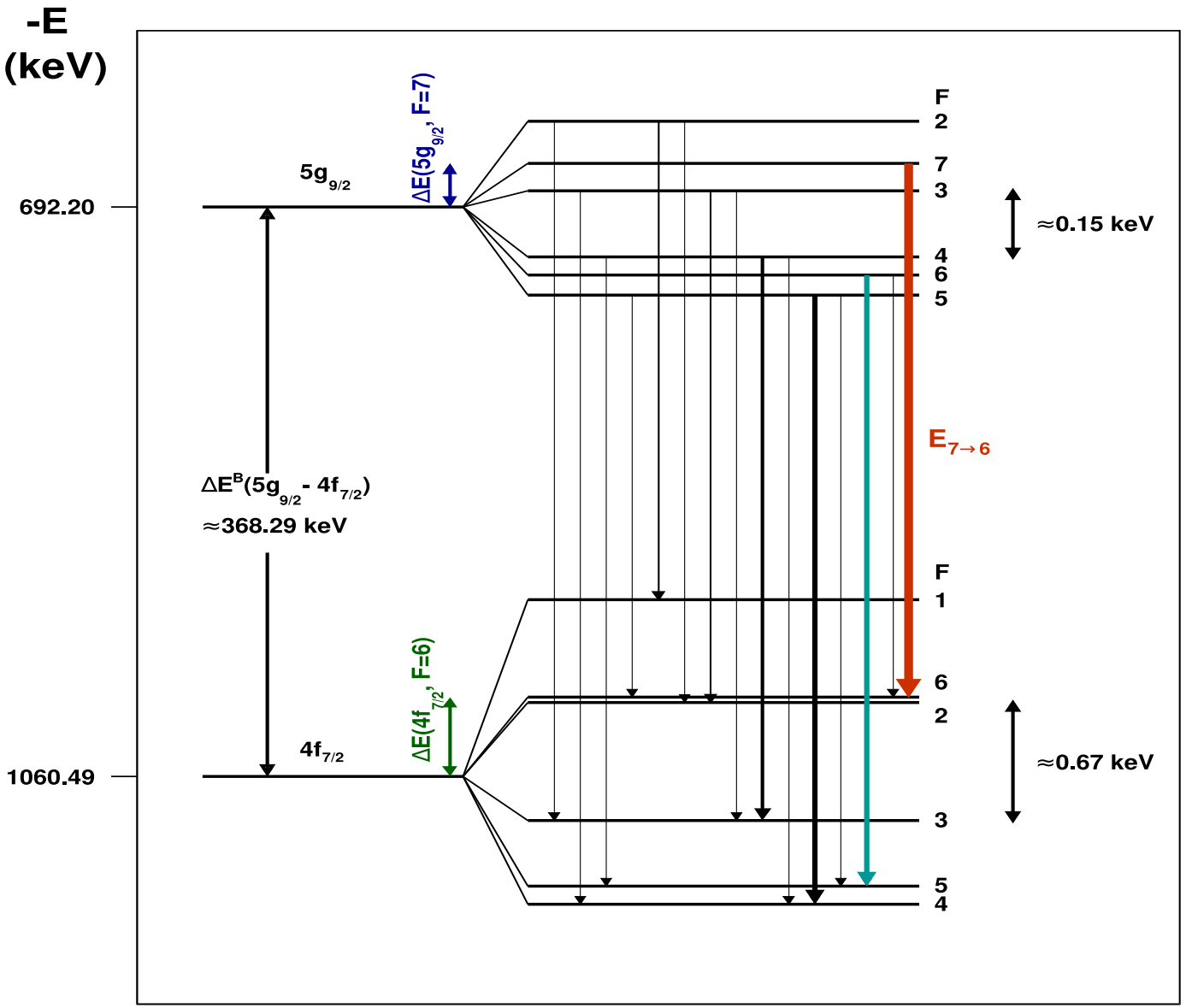

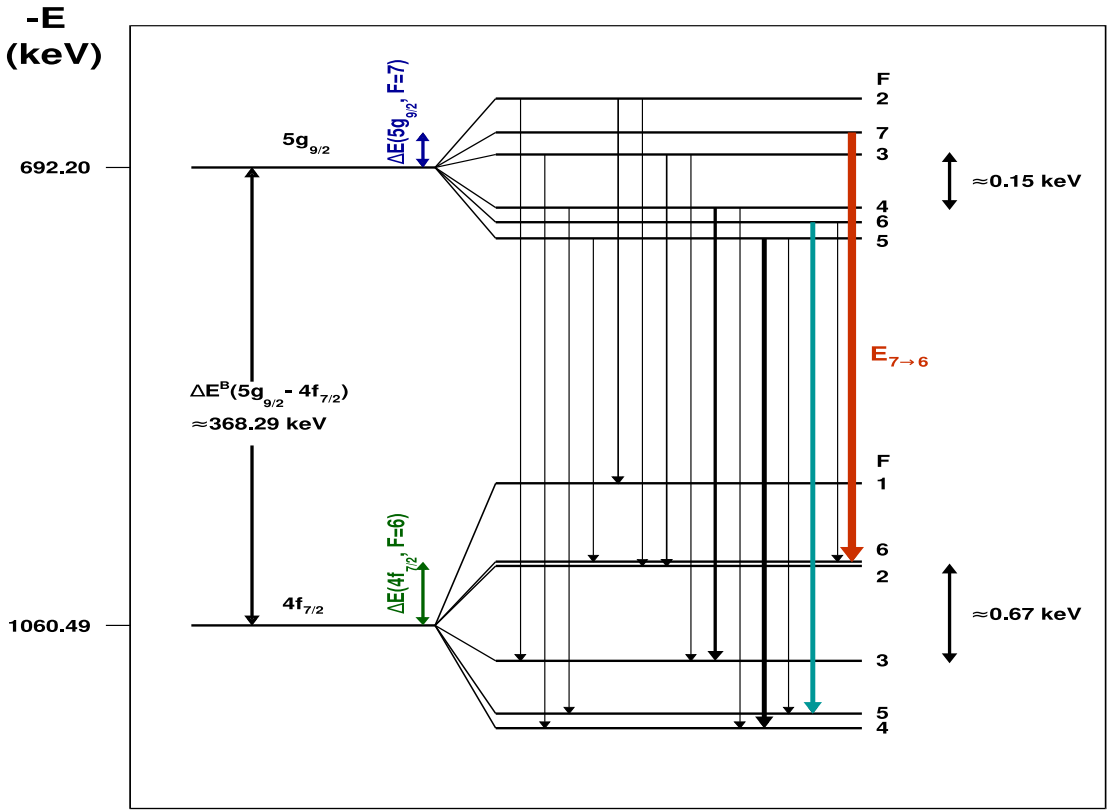

$$\left.\begin{aligned} E_{7\to6} &= E_7 - E_6' = \Delta E^B\left(5g_{9/2} - 4f_{7/2}\right) + \Delta E\left(5g_{9/2}, F=7\right) + \Delta E\left(4f_{7/2}, F=6\right) \\ E_{6\to5} &= E_6 - E_5' = \Delta E^B\left(5g_{9/2} - 4f_{7/2}\right) + \Delta E\left(5g_{9/2}, F=6\right) + \Delta E\left(4f_{7/2}, F=5\right) \end{aligned}\right\} \xRightarrow{(-)}$$

$$\Rightarrow E_{6\to5} = E_{7\to6} + \Delta E(\mu_N, Q)$$

$$\boxed{\begin{aligned} E_i &= E_0 + \Delta E(\mu_N, Q) \\ \Delta E(\mu_N, Q) &= Q^2 \cdot c_{quad_i} + Q \cdot c_{lin_i} + c_{const_i} \end{aligned}}$$

Experimental spectrum of the $5g - 4f$, $5f - 4d$ transitions in Re-185

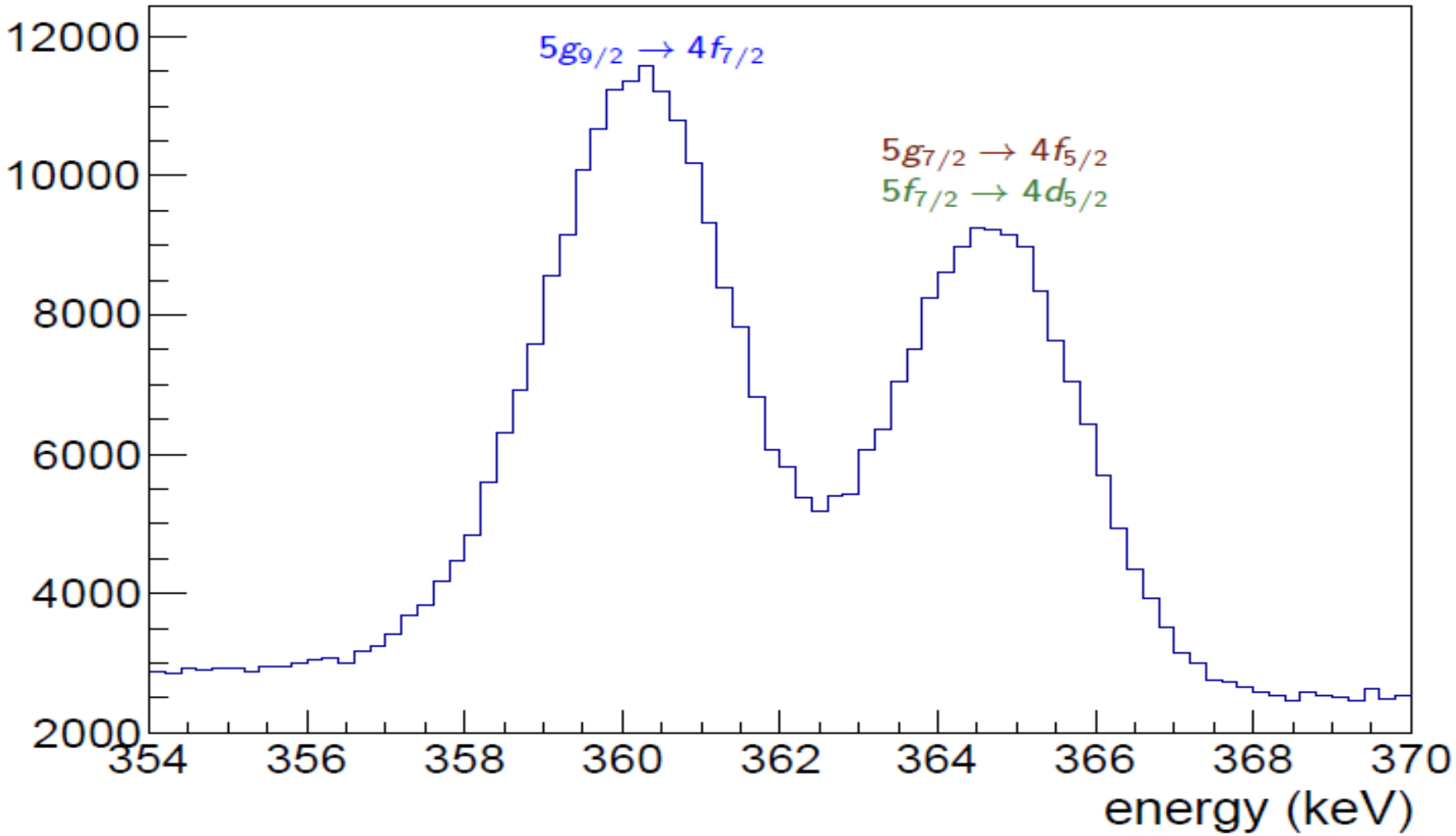

$5g \rightarrow 4f$, $5f \rightarrow 4d$ HFS in Re-185

Q = 2.21 b

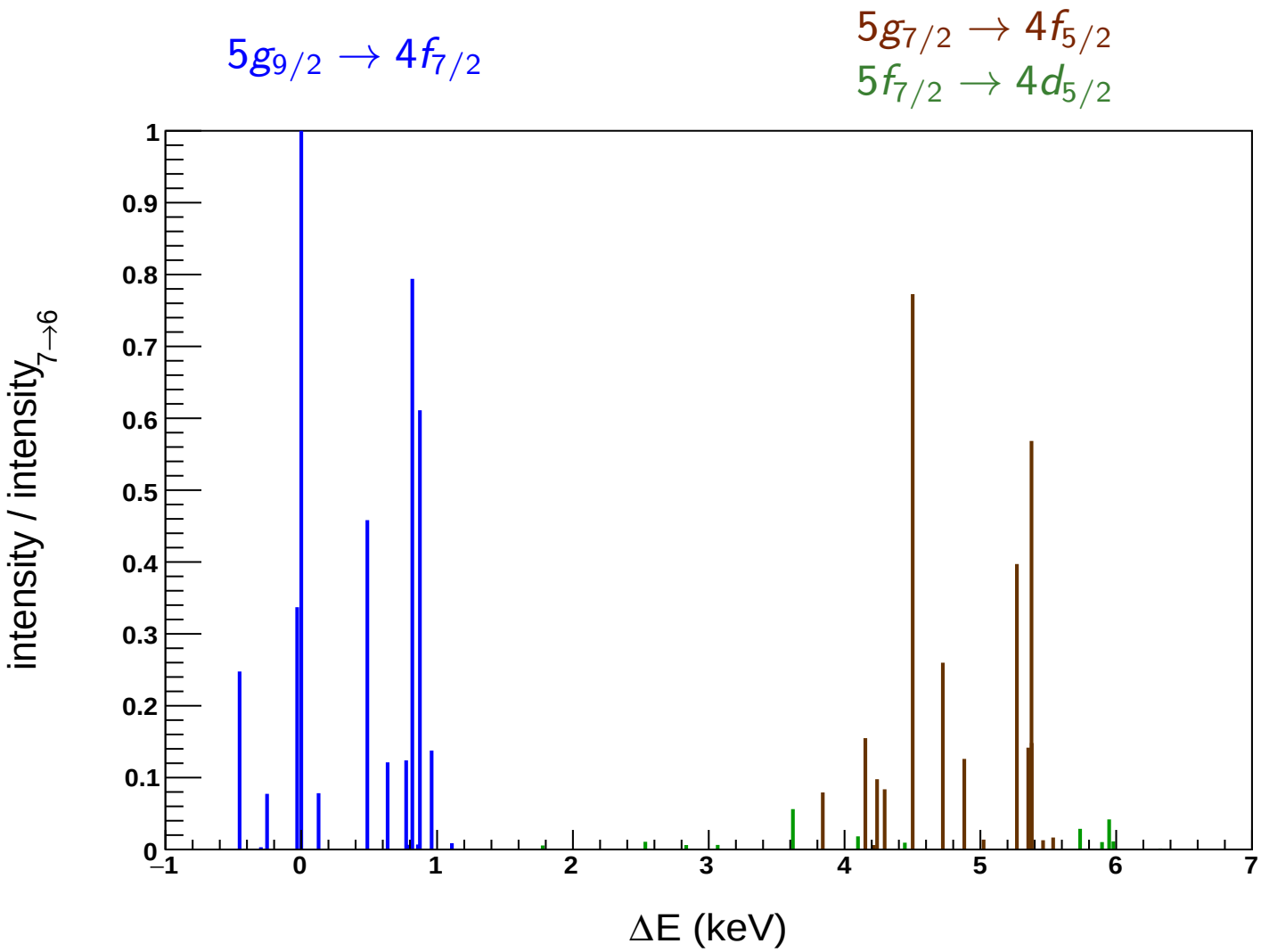

45 transitions

Absolute intensities scale:

$$\frac{I_{(5g_{7/2}\rightarrow 4f_{5/2})}}{I_{(5g_{9/2}\rightarrow 4f_{7/2})}} = 0.7727$$

$$\frac{I_{(5f_{7/2}\rightarrow 4d_{5/2})}}{I_{(5g_{9/2}\rightarrow 4f_{7/2})}} = 0.07886$$

***Theoretical energies and intensities calculated by N. Michel, Max-Planck-Institut für Kernphysik in Heidelberg**

Instrumental line-shape

1. Gaussian shape→ broadening of a line in an ideal detector (statistical fluctuations and electronic noise):

$$G(E) = \frac{1}{\sqrt{2\pi}\sigma} exp\left(-\frac{(E-m)^2}{2\sigma^2}\right)$$

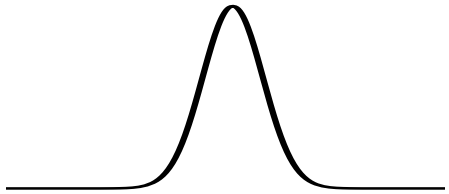

2. Hypermet shape → low-energy exponential tail (incomplete charge collection):

$$T(E) = \frac{1}{2\ b} \cdot exp\left(\frac{E-m}{b} + \frac{\sigma^2}{2b^2}\right) \cdot erfc\left(\frac{E-m}{\sqrt{2}\sigma} + \frac{\sigma}{\sqrt{2}b}\right)$$

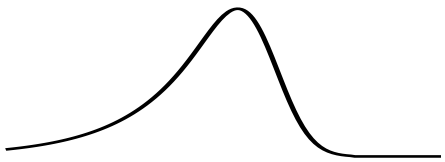

3. Step-like shelf shape → discontinuous background under each peak (accumulation of Compton scattering and pair production effects):

$$S(E) = \frac{A}{2} \cdot erfc\left(\frac{E-m}{\sqrt{2}\sigma}\right)$$

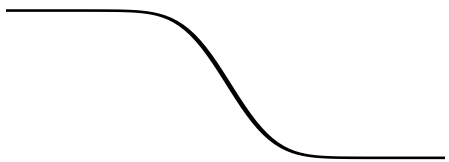

Energy spectra in Re-185 and Pb-208

Re-185

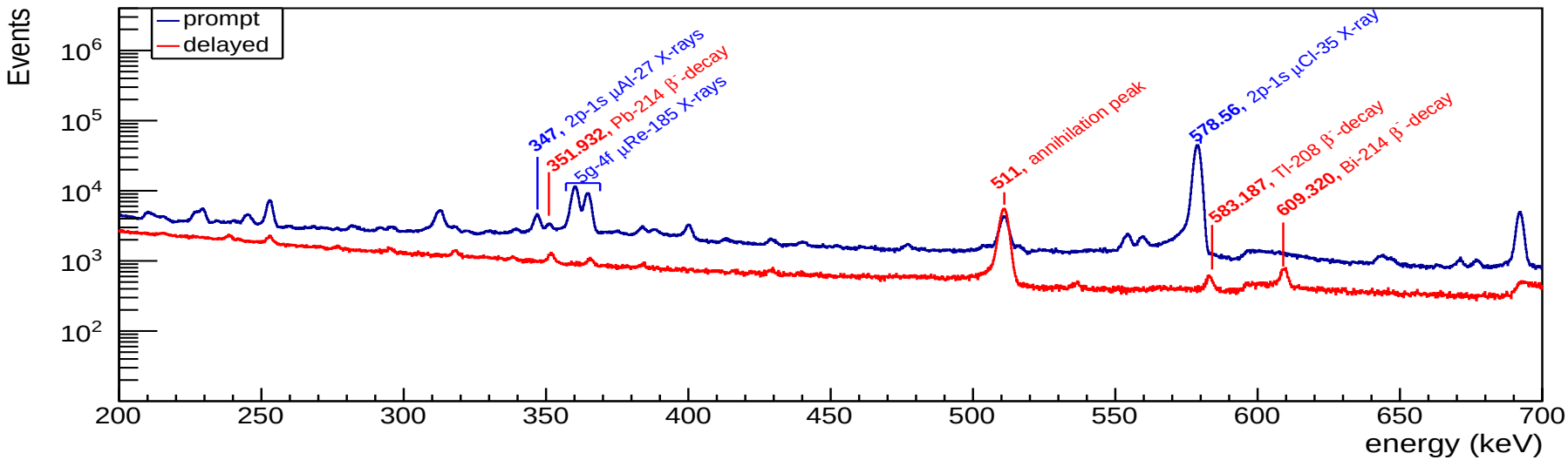

Pb-208

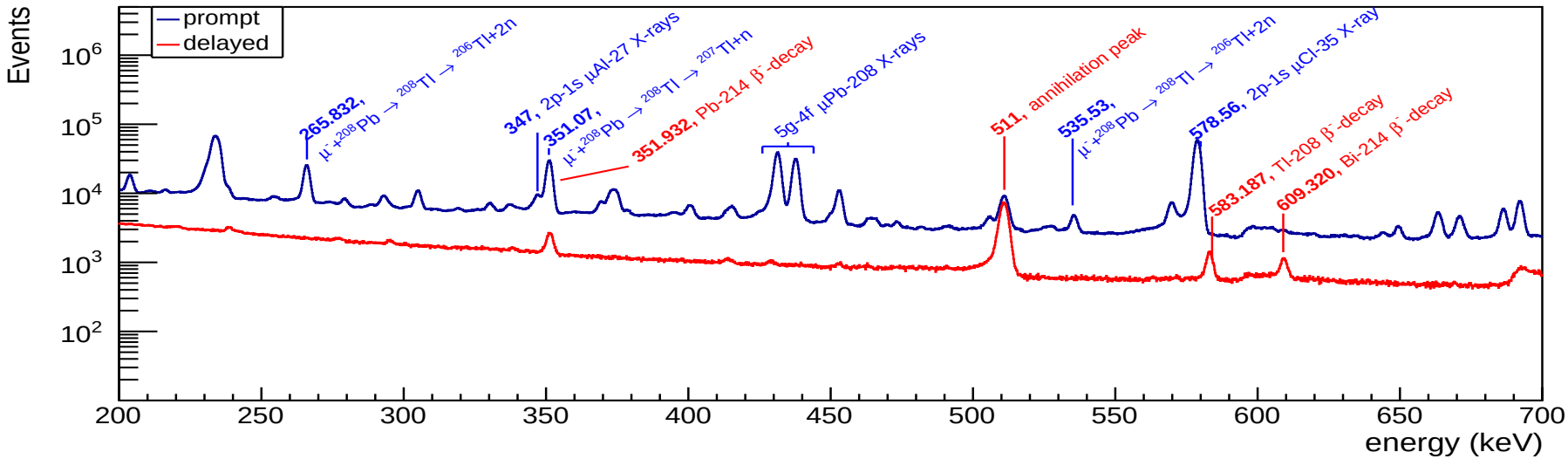

Lineshape fit

Total PDF in RooFit: $P(E) = N_{signal} \cdot (f_G\, G(E) + f_T\, T(E) + S(E)) + B$

265.832 keV

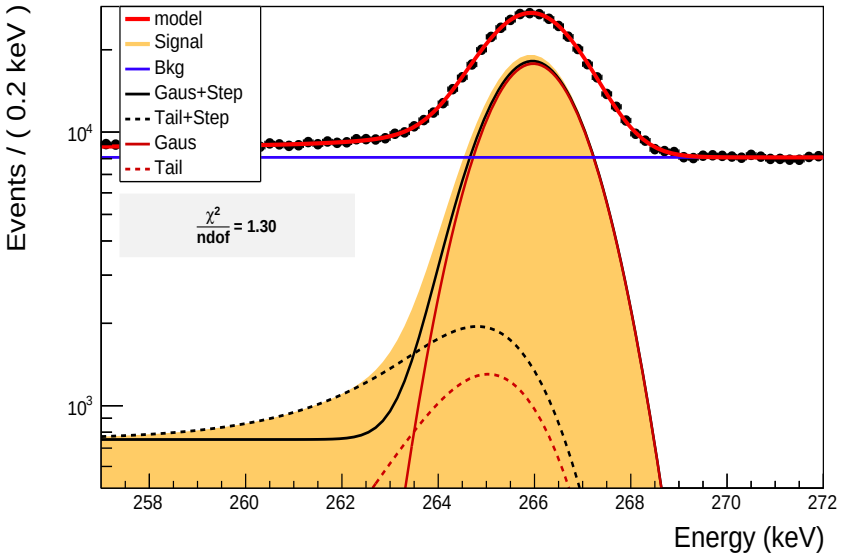

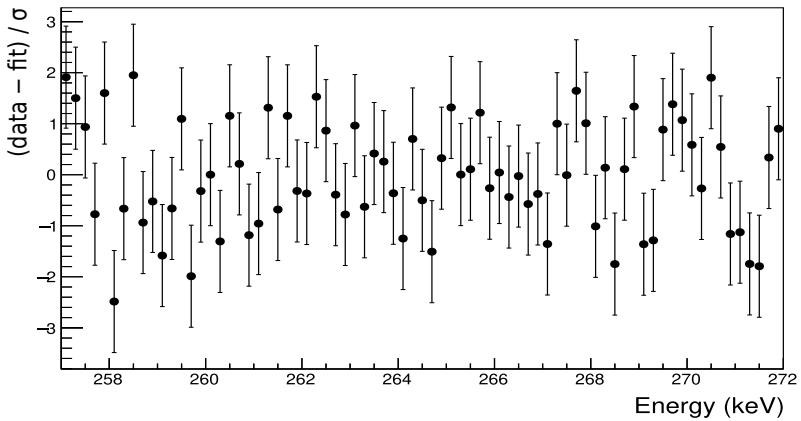

578.56 keV

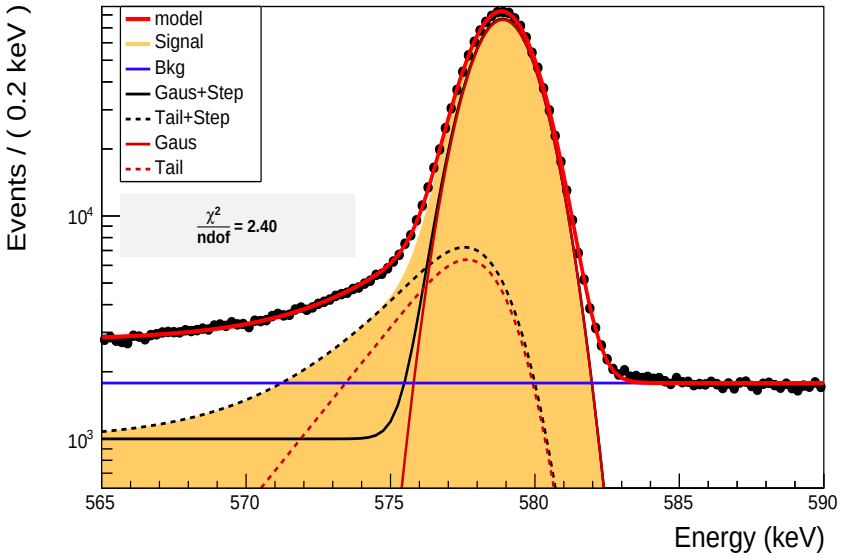

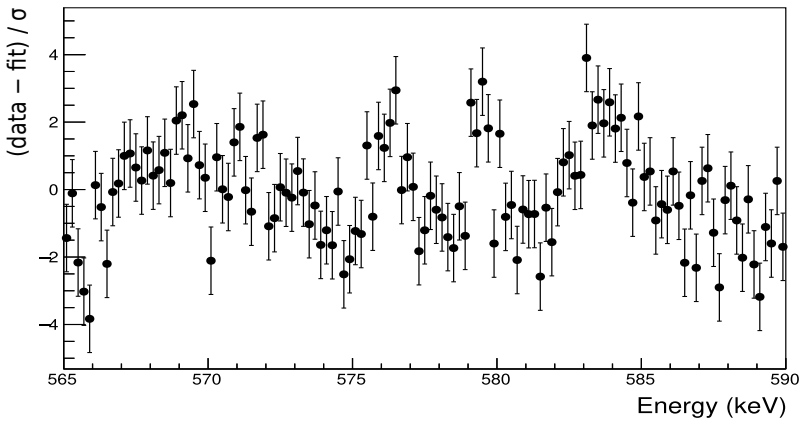

Lineshape fit

Lineshape parameters obtained from the fits:

Energy (keV)	$f_G = 1 - f_T$	b (keV)	m (keV)	σ (keV)	χ^2_{red}
265.832 ± 0.005	0.897 ± 0.009	1.7 ± 0.3	265.976 ± 0.006	0.995 ± 0.004	1.30
578.56 ± 0.30	0.867 ± 0.001	2.69 ± 0.06	578.886 ± 0.002	1.125 ± 0.001	2.40

Linear interpolation of sigma over energy [1]

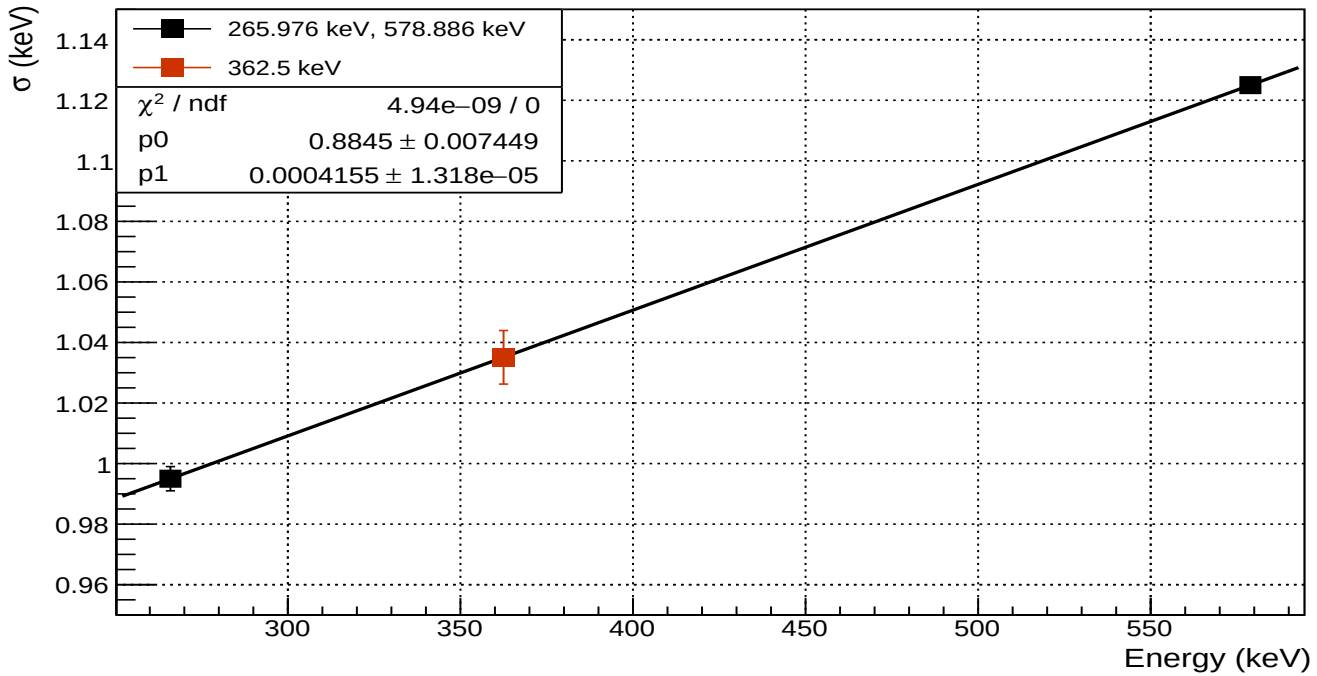

At 362.5 keV $\rightarrow \sigma = (1.035 \pm 0.009)$ keV

* Natural linewidth of 578.56 keV peak: 8 eV (minor change at the interpolated σ)

[1] G. F. Knoll, Radiation Detection and Measurement, 4th ed., Wiley, New York (2010)

Fit of the 5g-4f, 5f-4d HF transitions

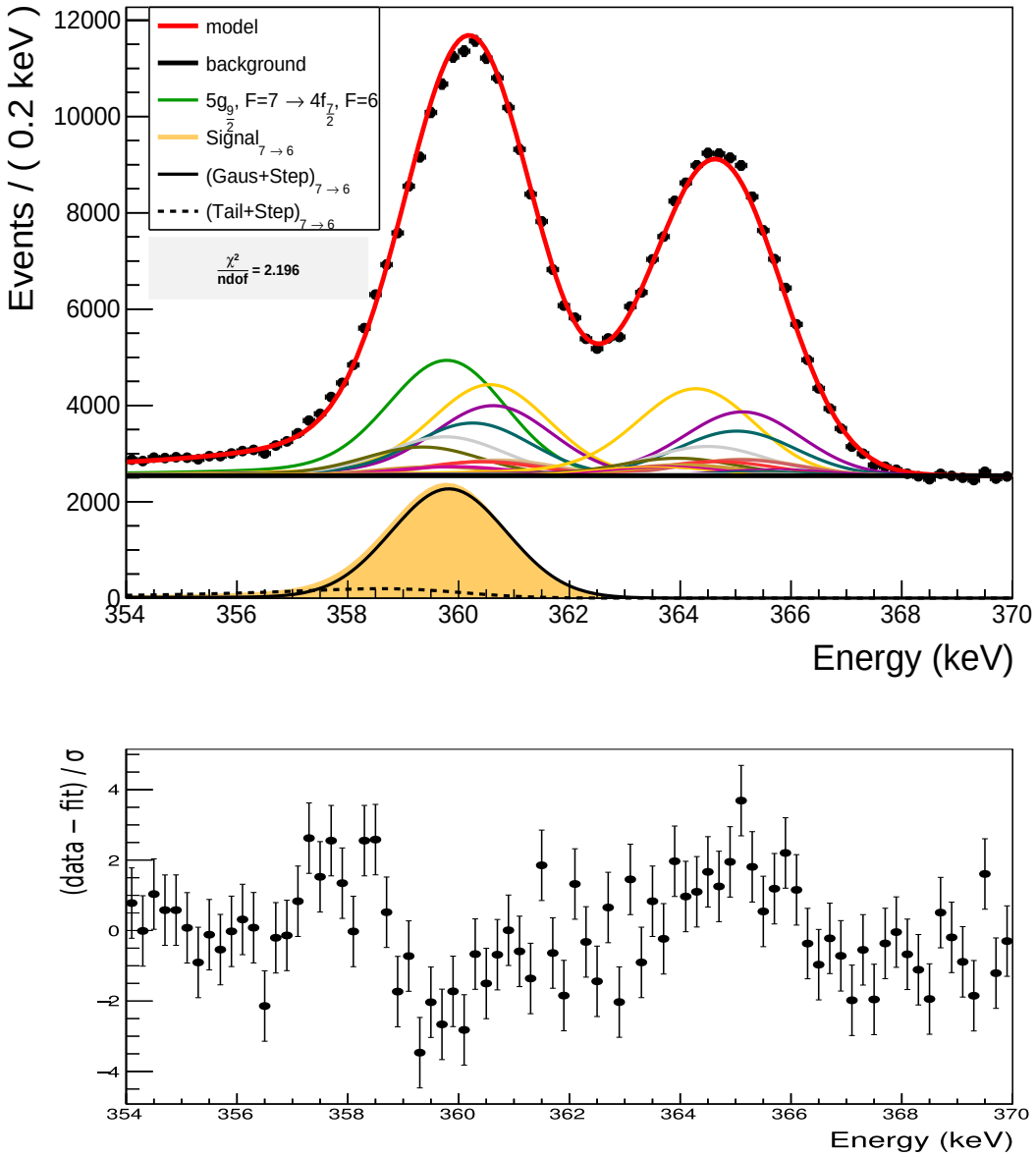

Fixed parameters:

- line-shape parameters (f_G, b, σ)
- ratio of absolute intensities

Fitted parameters:

- Q
- $E_{(5g_{9/2},\, F=7\to4f_{7/2},\, F=6)}$
- $N_{signal_{(\,5g_{9/2},\, F=7\to4f_{7/2},\, F=6)}}$
- A (step height)
- B (background constant)

Preliminary result

Result in this thesis:

$$\mathbf{Q = (2.12 \pm 0.04\ (stat) \pm 0.1\ (lineshape) \pm 0.04\ (cascade)\ )\,b}$$

Result obtained by similar analysis by means of muonic X-ray spectroscopy in the past[2]:

$$\mathbf{Q = (2.21 \pm 0.04)\,b}$$

[2] J. Konijn et al., Nucl. Phys. A **360**, 187 (1981)

Conclusions

1. Test of the efficiency of the detectors which serve to reduce the background due to Michel electrons in the HPGe detectors.

2. Development of the analysis tool for the fitting of the experimentally measured energies of the $5g - 4f$, $5f - 4d$ hyperfine transitions in Re-185.

3. Extraction of the quadrupole moment in Re-185 (preliminary).

Outlook

1. Further systematic study of the instrumental line-shape parameters
2. Analysis of the HFS in Re-185 with the other HPGe detector (20 % relative efficiency, better energy resolution)
3. Analysis of the HFS in Re-187

Thank you!

Backup Slides

Scintillation detectors' structure

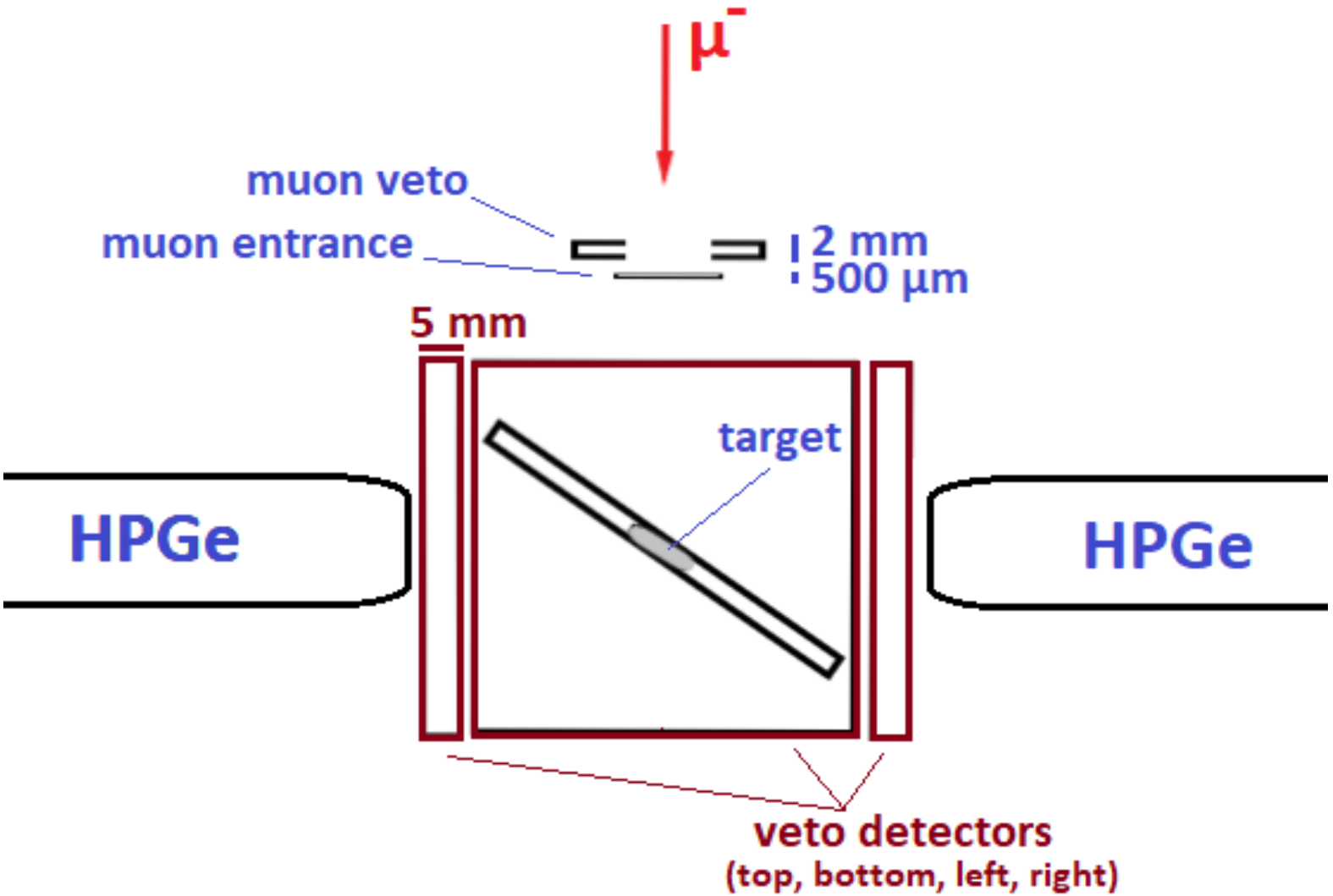

Dependence of cosmic muon flux on zenith anlge

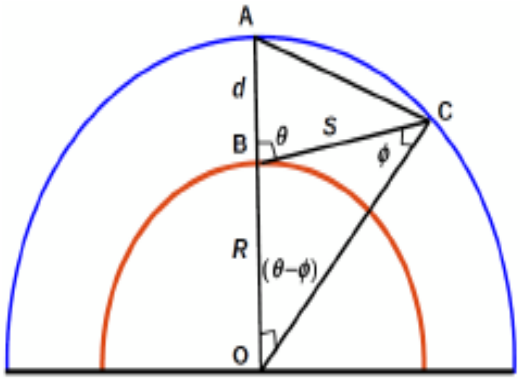

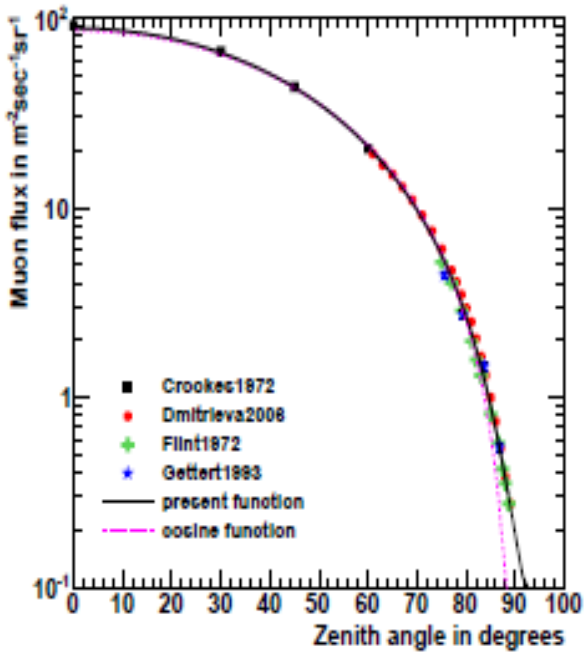

Figure: Cosmic muon flux as a function of zenith anlge at sea level.

$$\Phi(\theta) = I_0 cos^{n-1}(\theta)$$

Absolute efficiency of the veto detectors in their different quadrants

$veto_i$	$quad_1$	$quad_2$	$quad_3$	$quad_4$	total
$veto_T$	0.999 ± 0.016	0.998 ± 0.017	0.998 ± 0.016	0.998 ± 0.019	0.998 ± 0.008
$veto_R$	0.960 ± 0.015	0.940 ± 0.014	0.960 ± 0.015	0.938 ± 0.017	0.950 ± 0.008
$veto_{No1}$	0.932 ± 0.011	0.970 ± 0.011	0.951 ± 0.011	0.979 ± 0.013	0.957 ± 0.006
$veto_B$	0.999 ± 0.011	0.998 ± 0.011	0.998 ± 0.011	0.998 ± 0.013	0.998 ± 0.006
$veto_{No2}$	0.956 ± 0.011	0.975 ± 0.011	0.968 ± 0.011	0.984 ± 0.013	0.970 ± 0.006
$veto_L$	0.998 ± 0.011	0.997 ± 0.011	0.997 ± 0.011	0.998 ± 0.013	0.997 ± 0.006
$veto_{No3}$	0.999 ± 0.011	0.998 ± 0.011	0.999 ± 0.011	0.999 ± 0.013	0.999 ± 0.006

Pmt single energy spectra

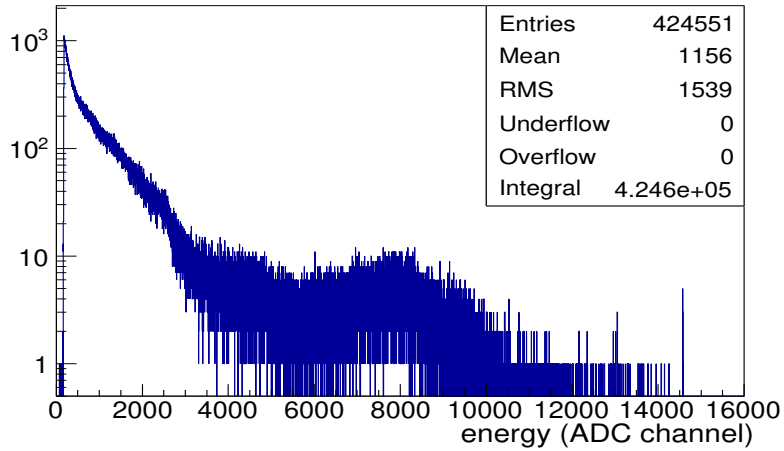

pmt_1

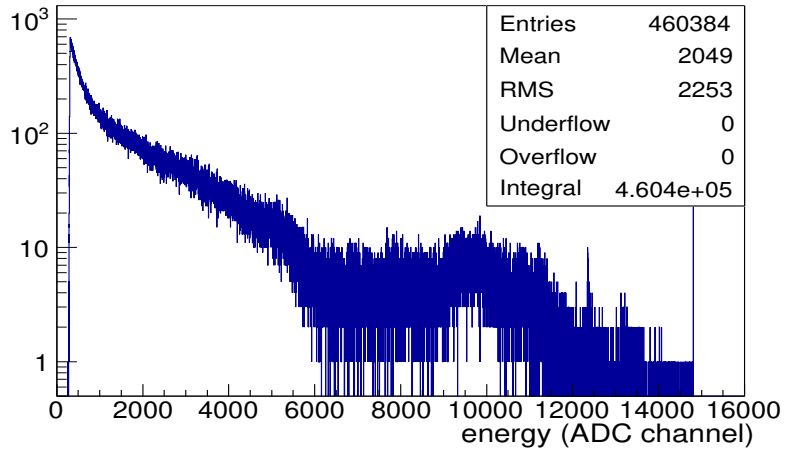

pmt_2

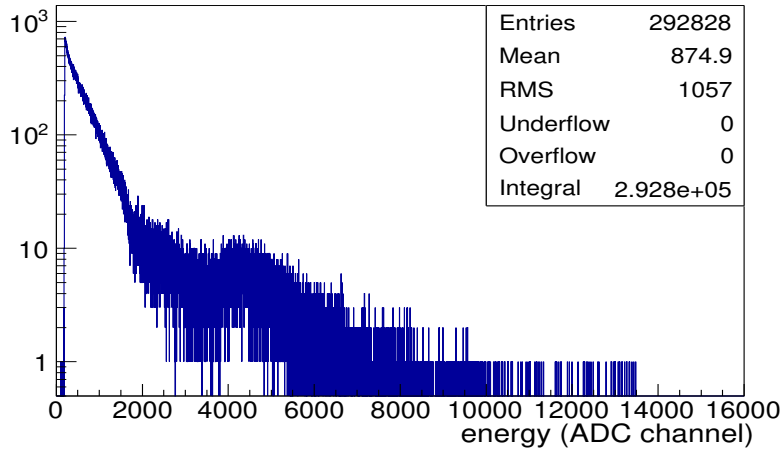

pmt_3

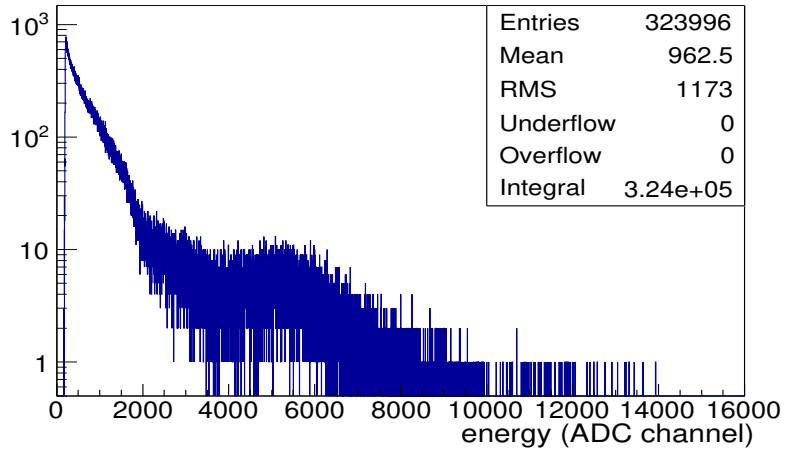

pmt_4

Time difference distributions between pmt and veto

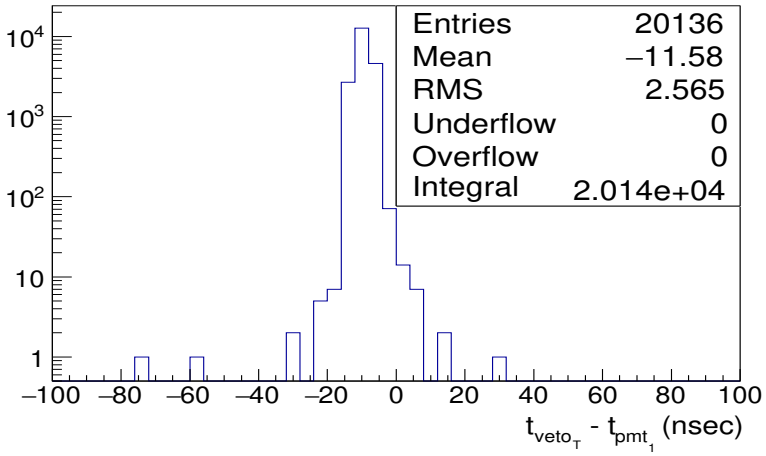

$t_{veto_T} - t_{pmt_1}$

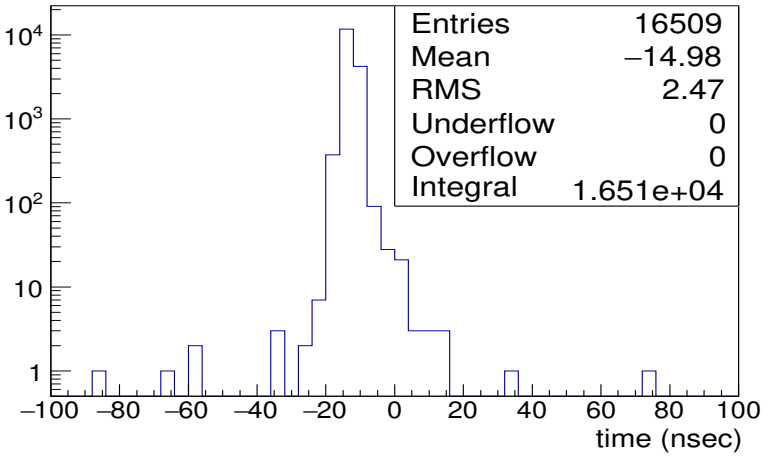

$t_{veto_T} - t_{pmt_2}$

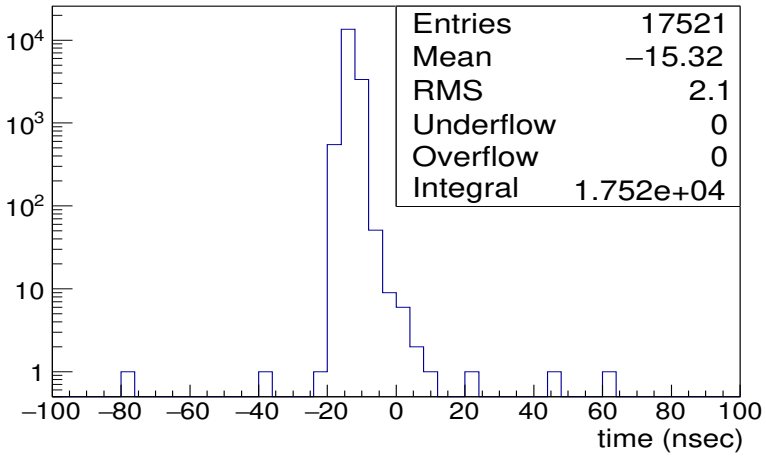

$t_{veto_T} - t_{pmt_3}$

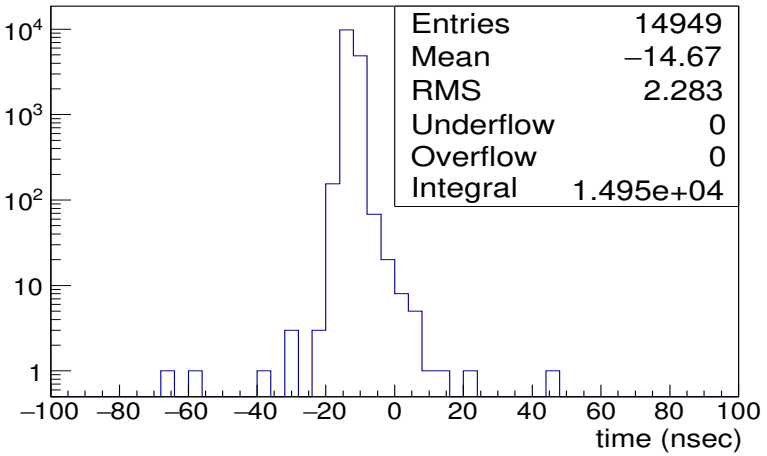

$t_{veto_T} - t_{pmt_4}$

Veto coincidence energy spectra without energy cuts

	vetoT	vetoR	vetoNo1	vetoB
quad1	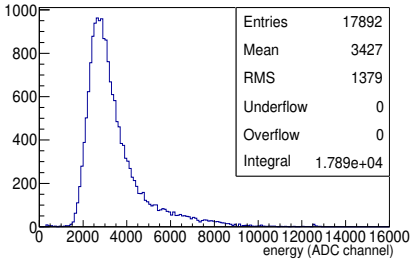	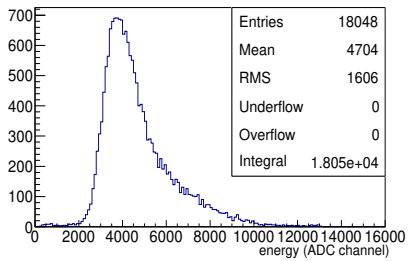	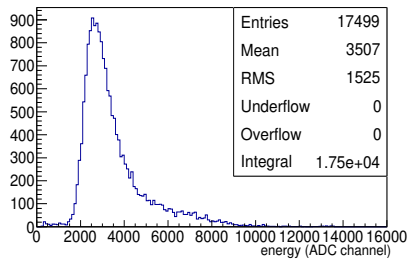	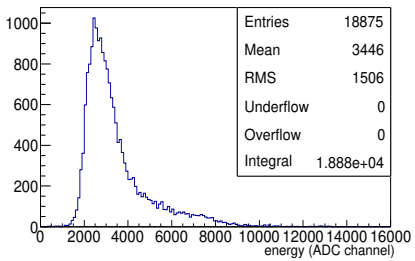
quad2	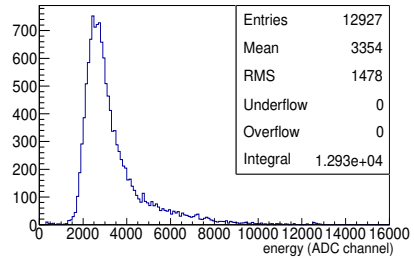	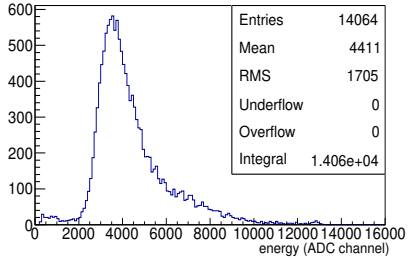	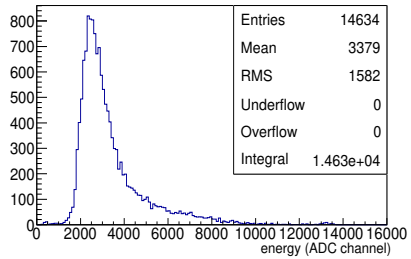	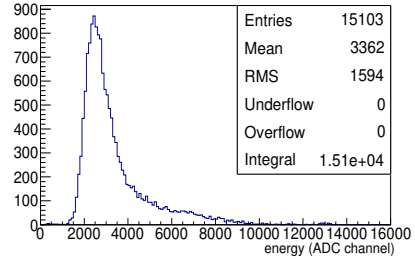
quad3	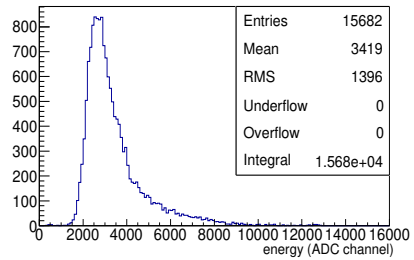	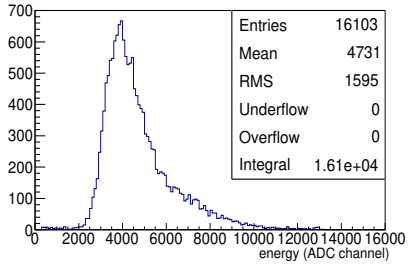	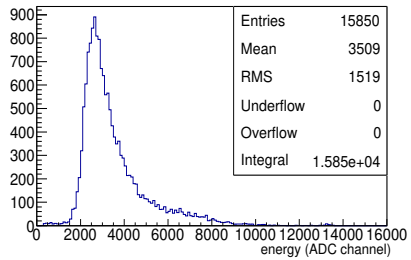	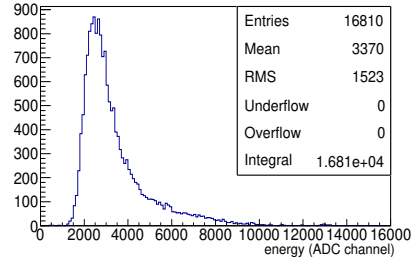
quad4	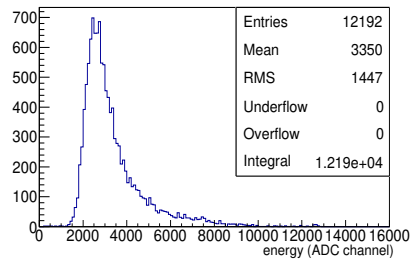	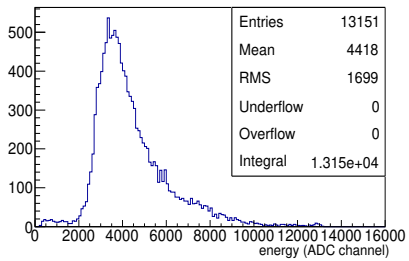	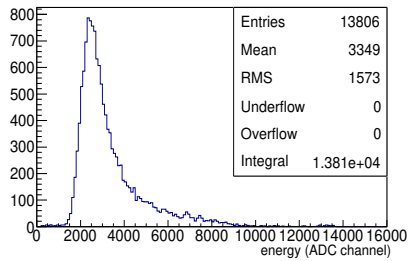	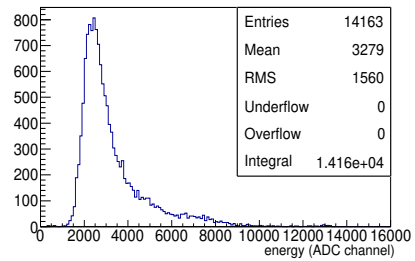

Veto coincidence energy spectra without energy cuts

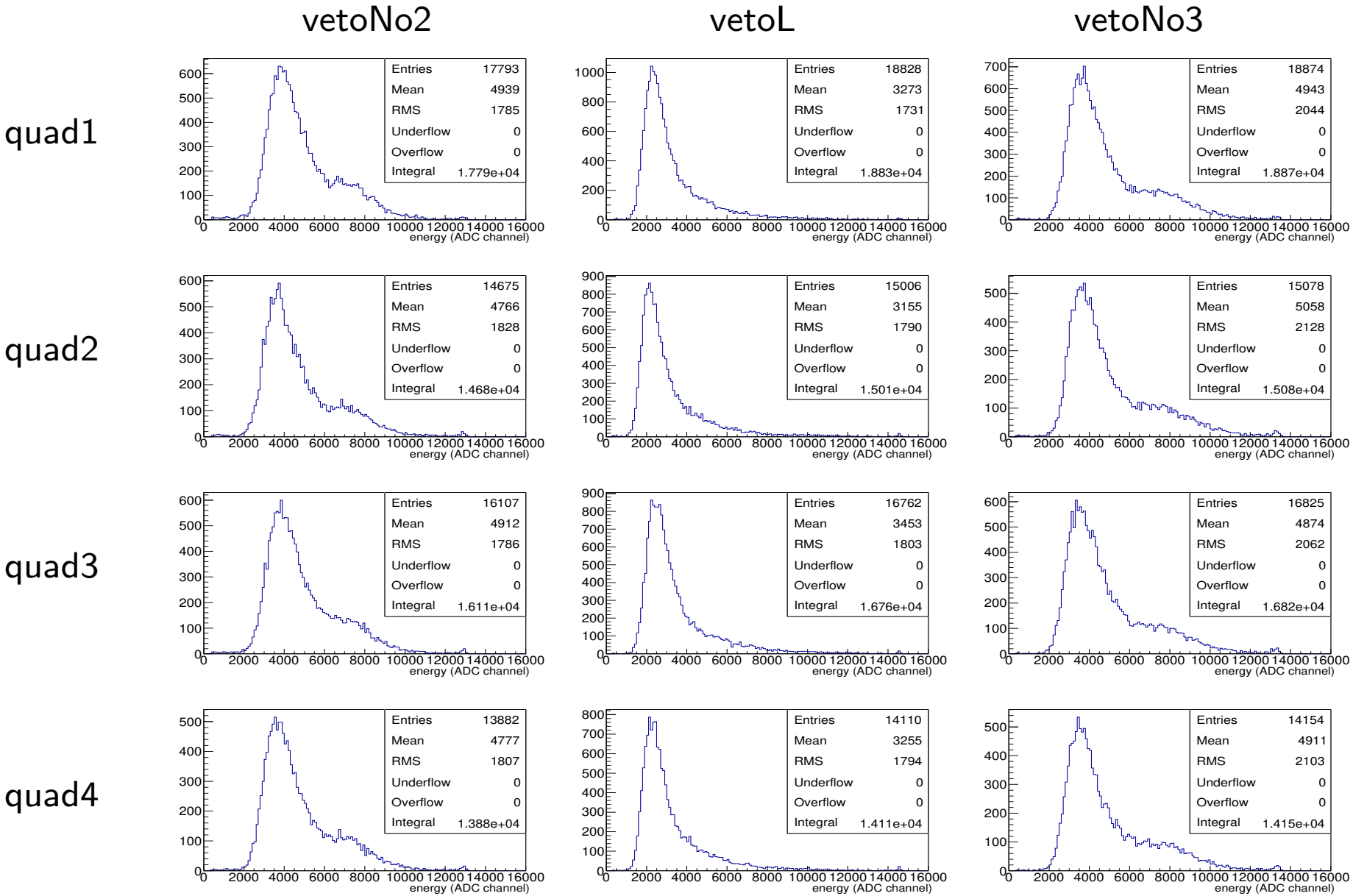

Coincidence spectra when pmt_i in coincidence with pmt_1

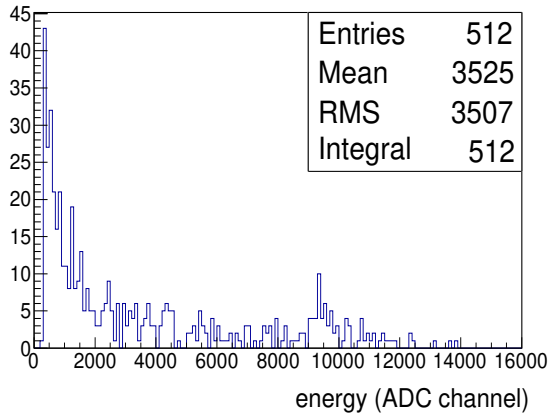

pmt_2

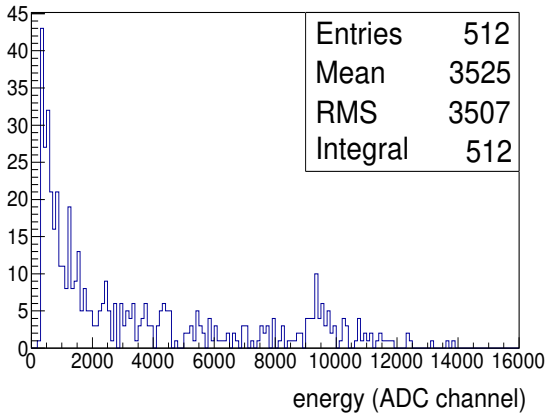

pmt_3

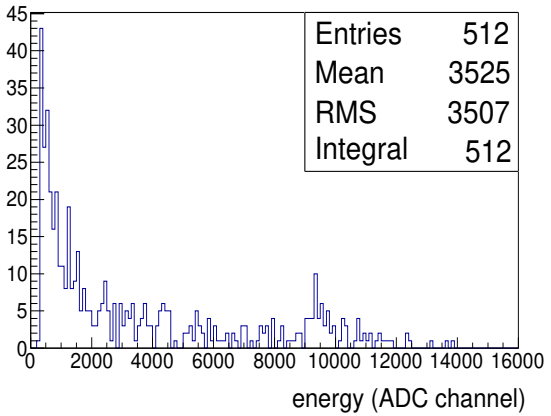

pmt_4

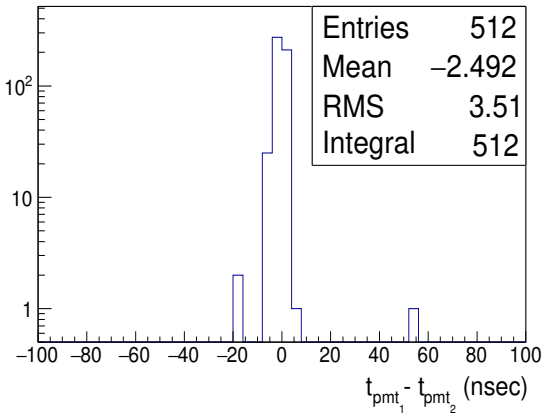

$t_{pmt_1} - t_{pmt_2}$

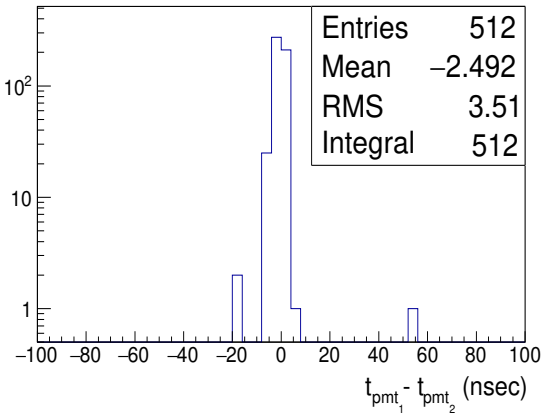

$t_{pmt_1} - t_{pmt_3}$

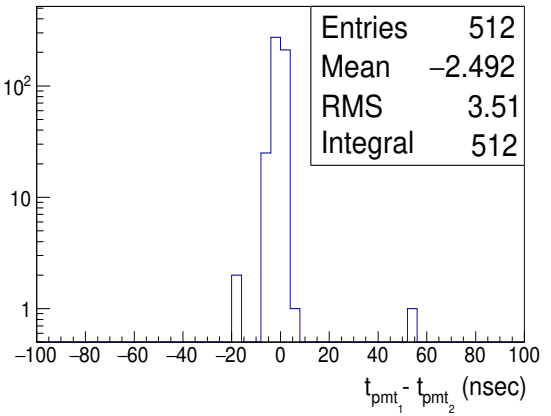

$t_{pmt_1} - t_{pmt_4}$

Data offline analysis

$pmt_{2,3,4}$ in coincidence with pmt_1

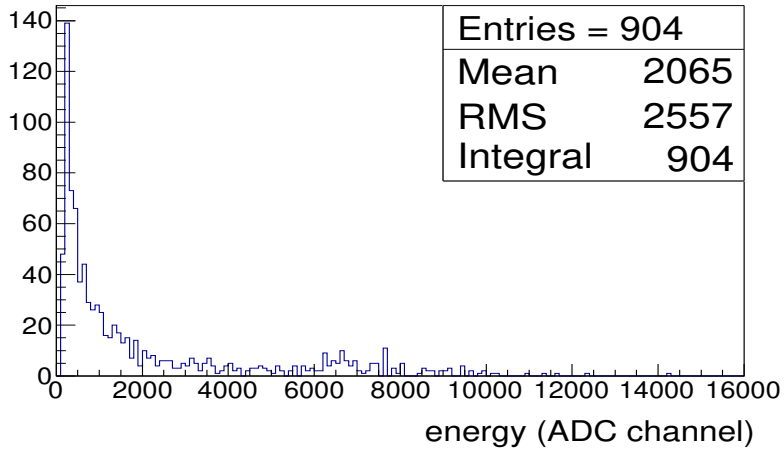

pmt_1

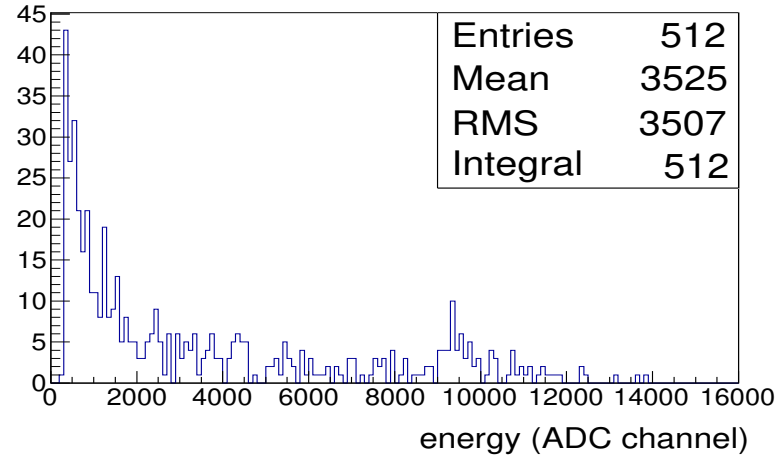

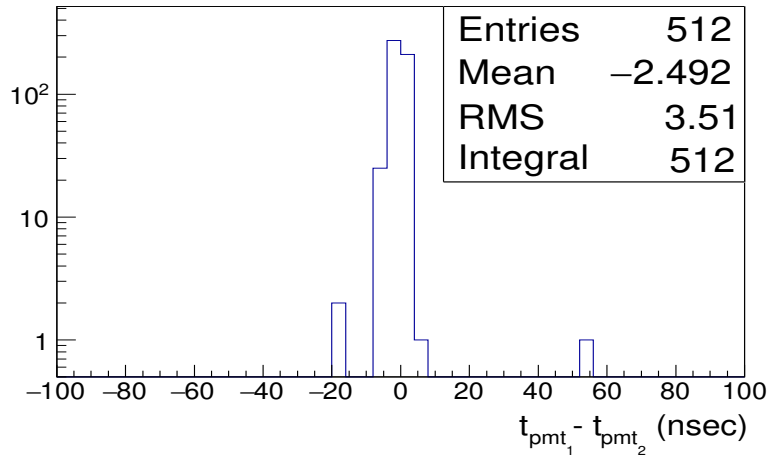

pmt_2

Data offline analysis

$pmt_{2,3,4}$ in coincidence with pmt_1

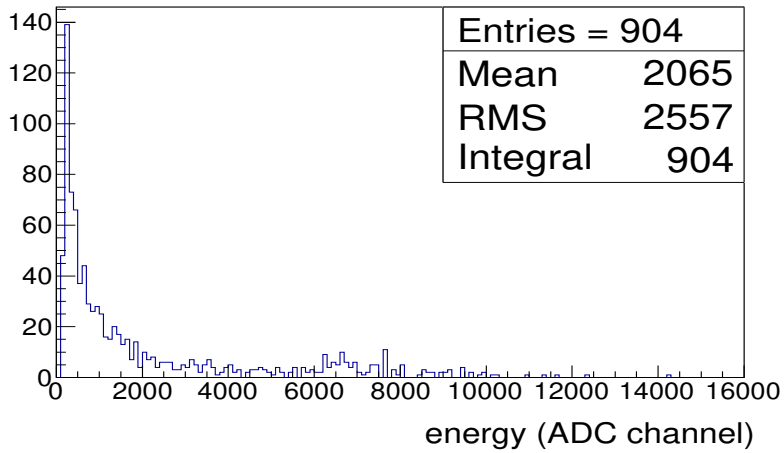

pmt_1

For $E_{pmt_1} < 4000$ ADC channel:

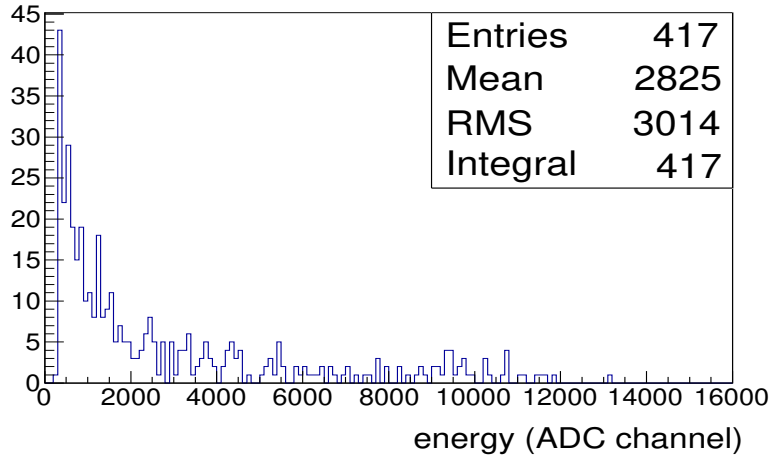

For $E_{pmt_1} > 4000$ ADC channel:

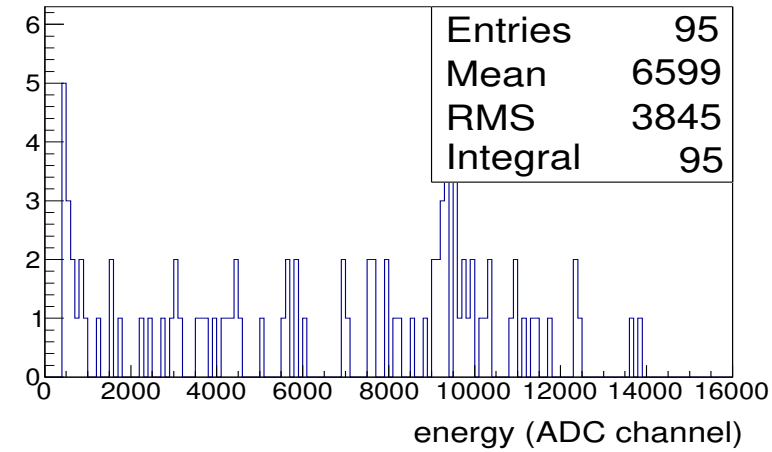

pmt_2

Energy spectra $veto_i$ in coincidence with $veto_T$

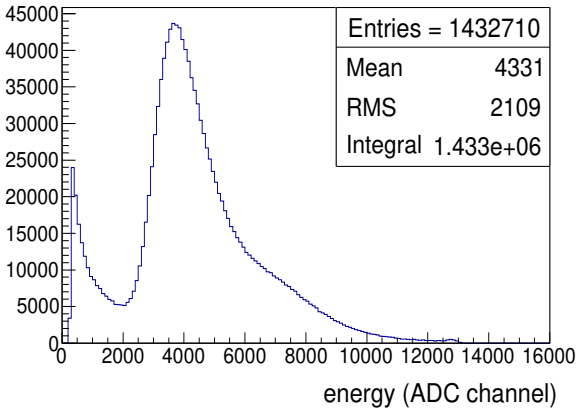

$veto_R$

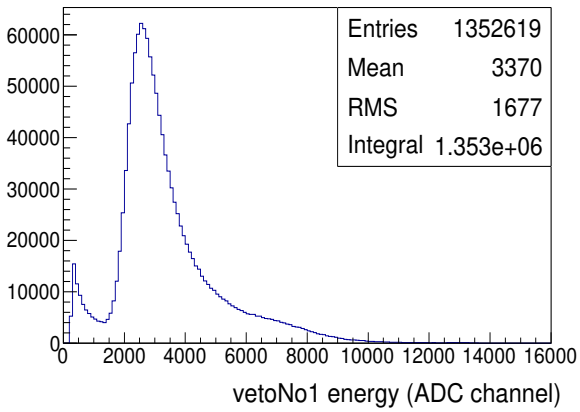

$veto_{No1}$

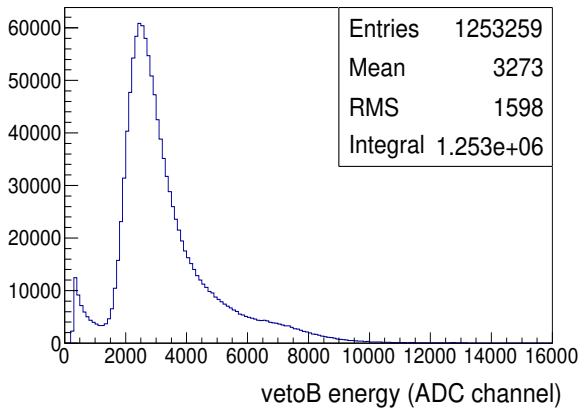

$veto_B$

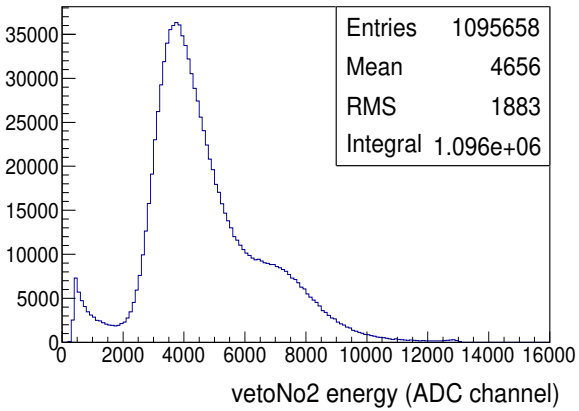

$veto_{No2}$

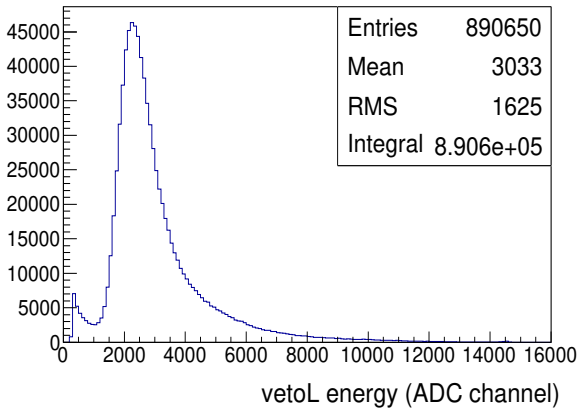

$veto_L$

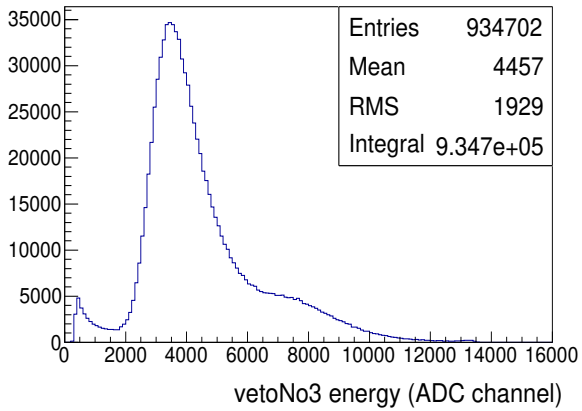

$veto_{No3}$

Time difference distributions $veto_i$ in coincidence with $veto_T$

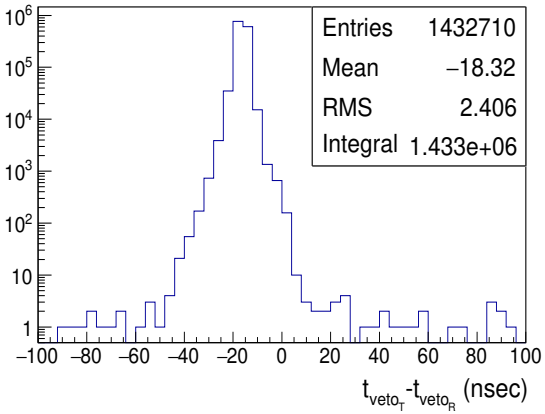

$t_{veto_T} - t_{veto_R}$

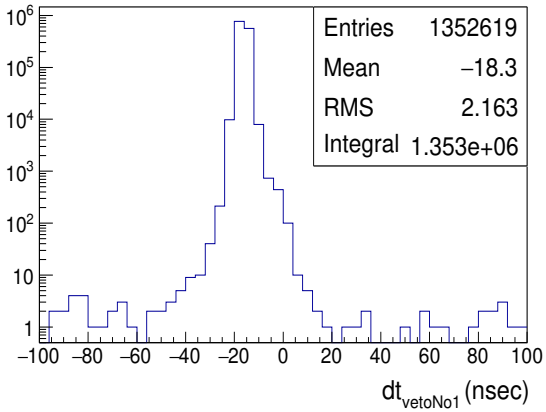

$t_{veto_T} - t_{veto_{No1}}$

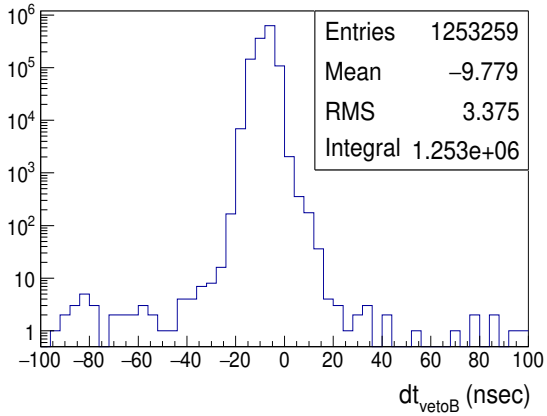

$t_{veto_T} - t_{veto_B}$

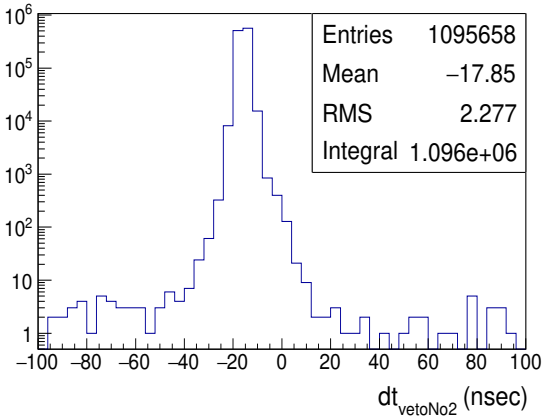

$t_{veto_T} - t_{veto_{No2}}$

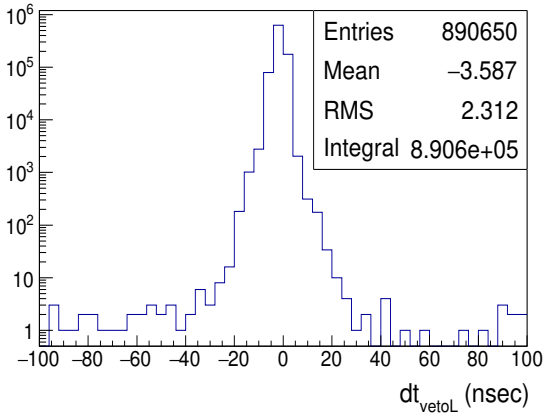

$t_{veto_T} - t_{veto_L}$

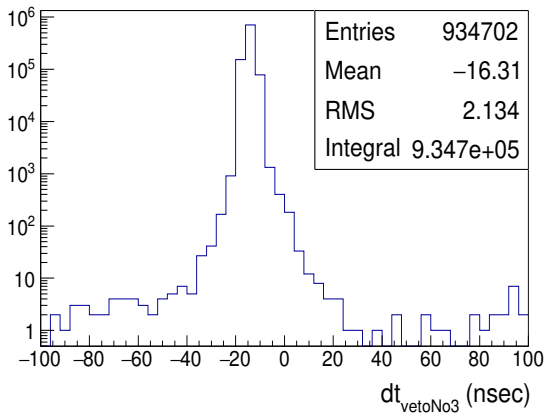

$t_{veto_T} - t_{veto_{No3}}$

Veto coincidence energy spectra when $veto_i$ in coincidence with pmt_j

	vetoR	vetoNo1	vetoB
quad1	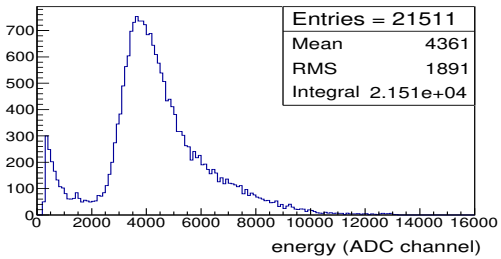	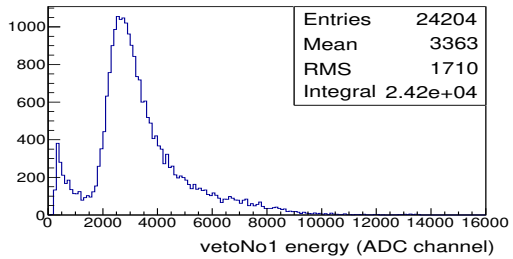	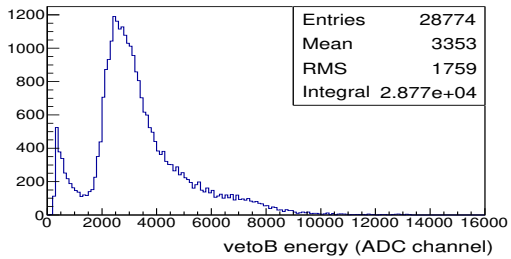
quad2	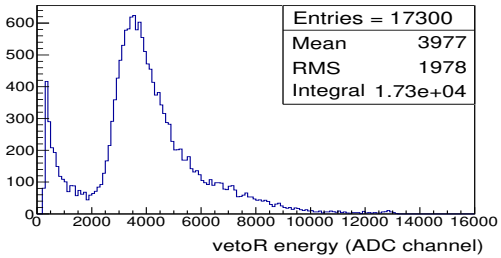	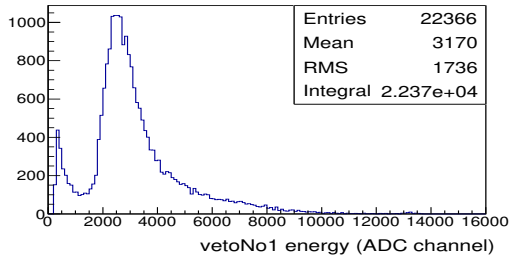	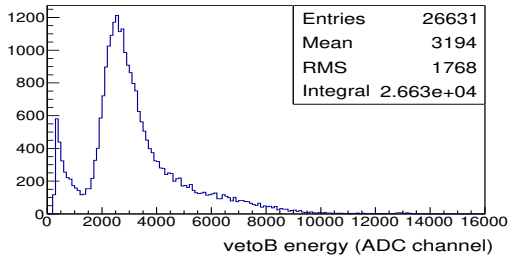
quad3	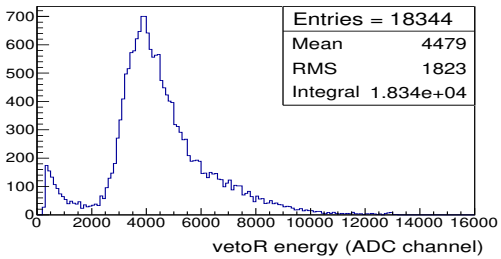	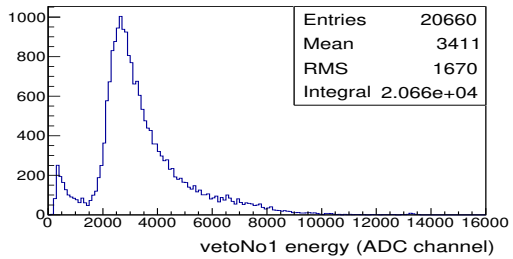	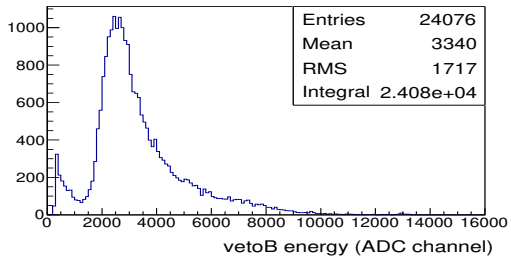
quad4	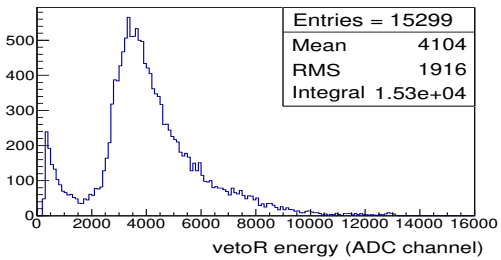	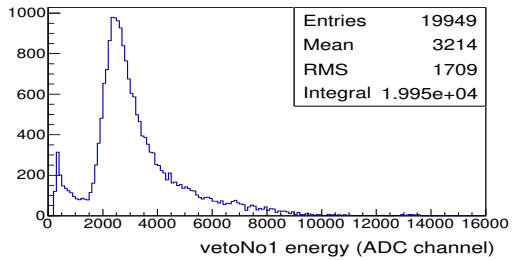	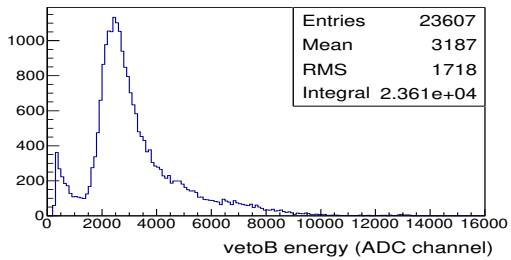

Veto coincidence energy spectra when $veto_i$ in coincidence with pmt_j

	vetoNo2	vetoL	vetoNo3
quad1	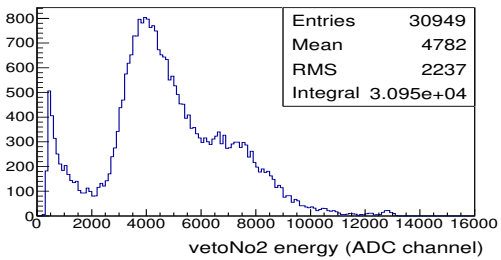	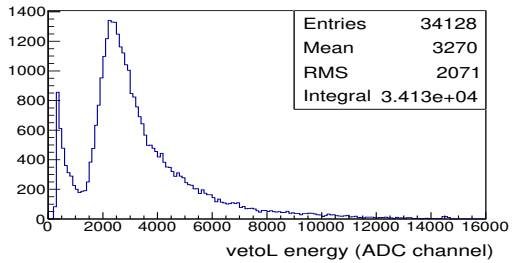	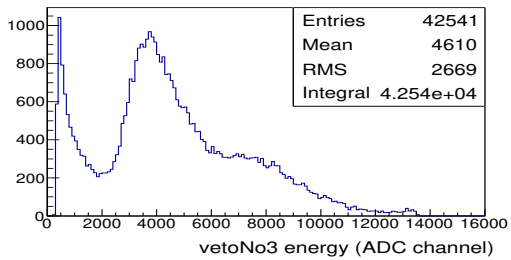
quad2	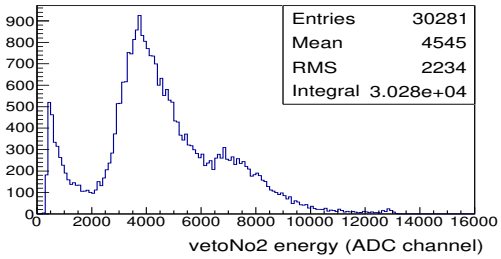	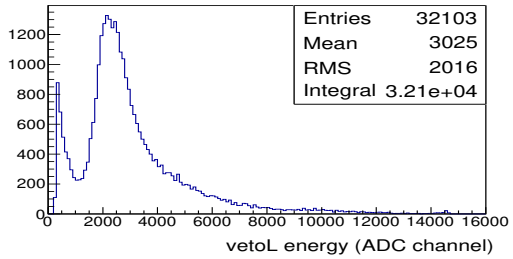	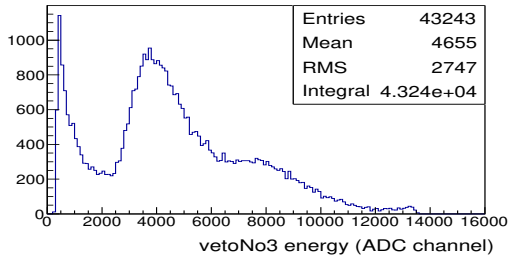
quad3	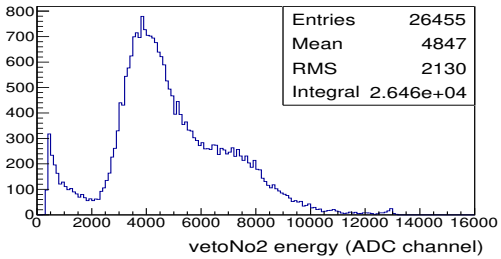	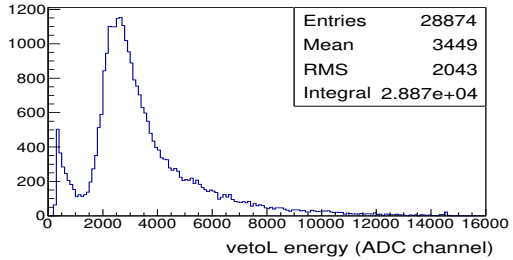	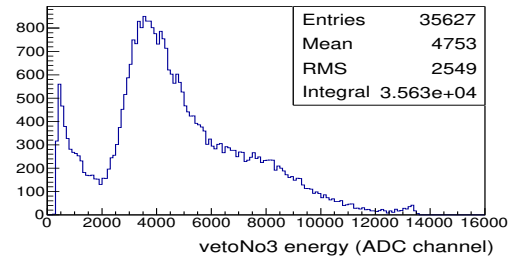
quad4	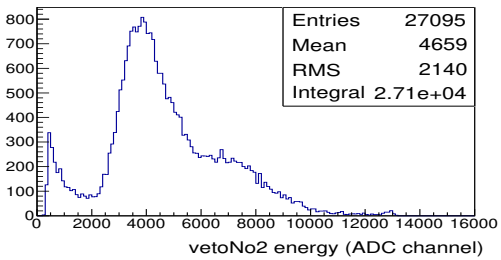	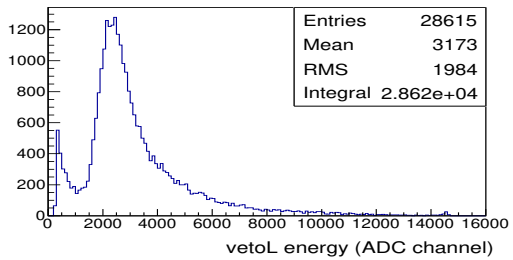	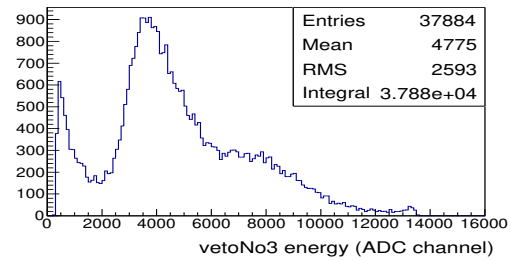

Veto time difference distribution when $veto_i$ in coincidence with pmt_j

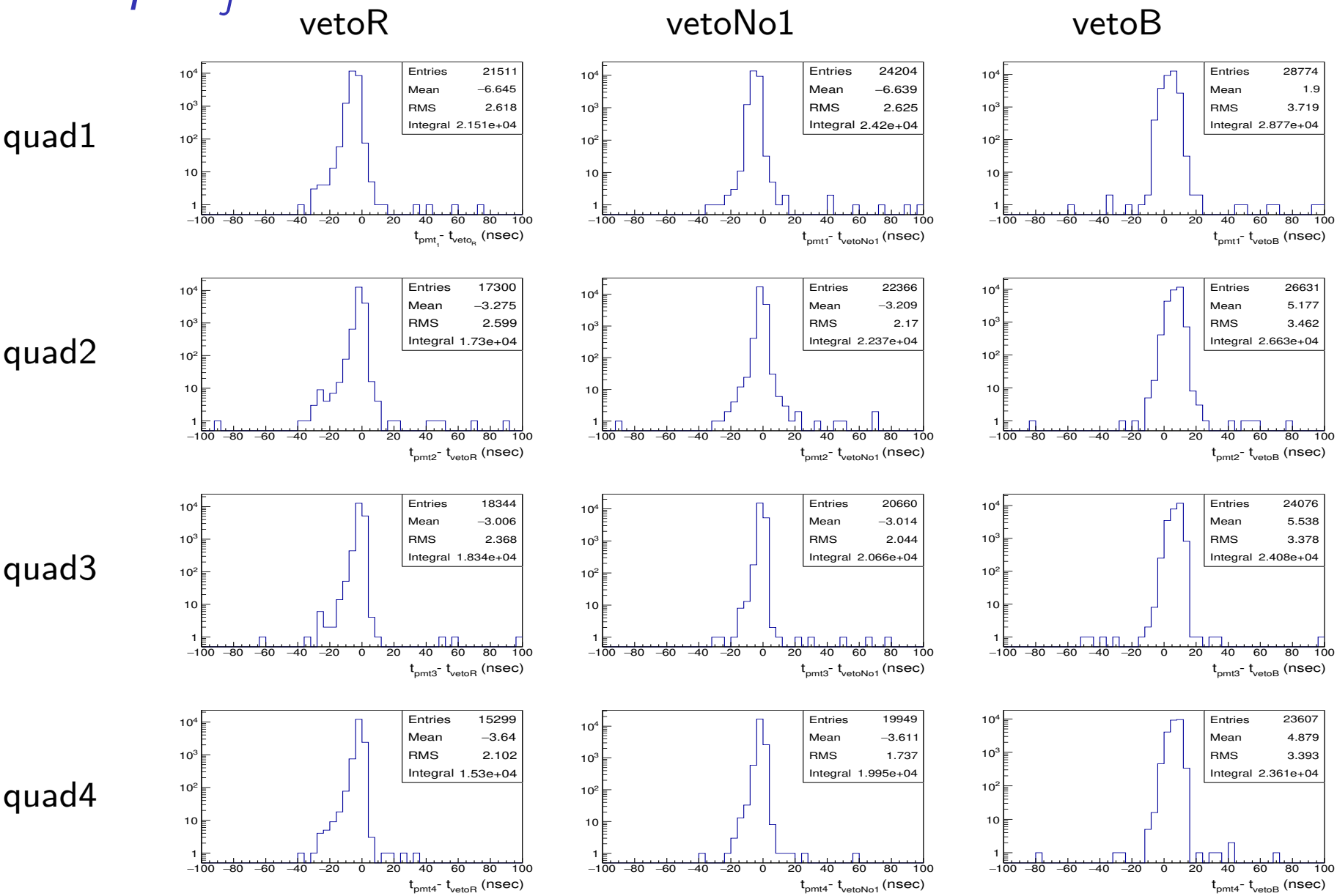

Veto time difference distribution when $veto_i$ in coincidence with pmt_j

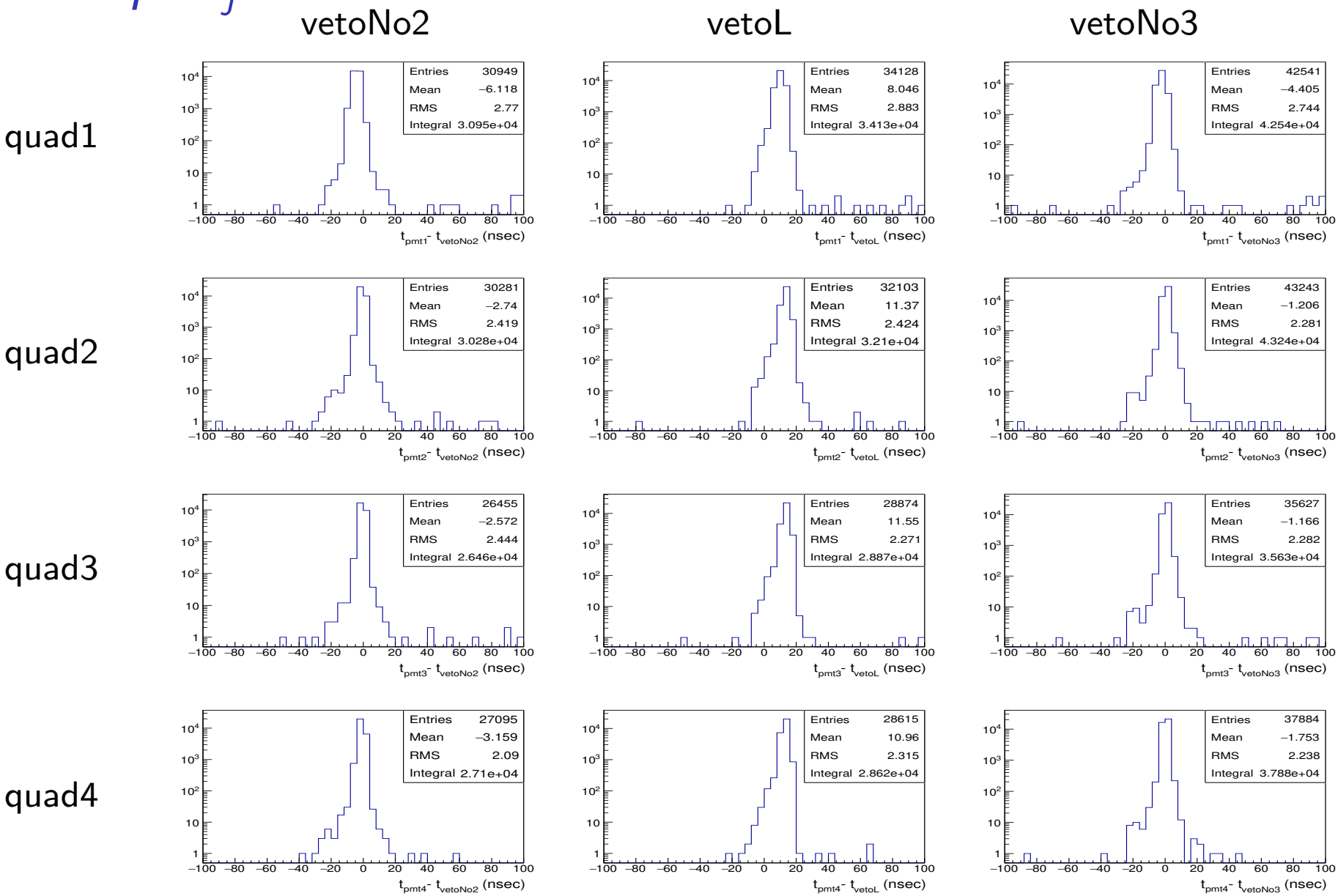

Fine and Hyperfine transitions

Fine structure from the muon muon spin-orbit coupling:

$$\vec{J} = \vec{L} + \vec{S} \tag{1}$$

Selection rules: $\Delta L = \pm 1,\ \Delta J = 0, \pm 1 \longrightarrow$

$$\begin{aligned} 5g_{9/2} &\rightarrow 4f_{7/2} \\ 5g_{7/2} &\rightarrow 4f_{5/2} \\ 5f_{7/2} &\rightarrow 4d_{5/2} \\ 5f_{5/2} &\rightarrow 4d_{3/2} \end{aligned}$$

Hyperfine structure from the nuclear spin-muon total angular momentum coupling:

$$\vec{F} = \vec{I} + \vec{J} \tag{2}$$

$I(^{185}Re) = 5/2$ and $\Delta F = 0, \pm 1$

Energy levels in μRe-185

The total Hamiltonian for a muon bound to a nucleus:

$$H = H_N + H_\mu + H_{\mu-N} \tag{3}$$

Charge distribution in a multipole expansion:

$$\rho(\overrightarrow{r}) = \rho_0(r) + \sum_{lm} \rho_{lm} Y_{lm}(\theta, \phi) \tag{4}$$

spherical part: gross and fine structure
non-spherical part: hyperfine structure

Intrinsic quadrupole moment of the nucleus:

$$Q_0 = 2\sqrt{\frac{4\pi}{5}} \int \rho(\overrightarrow{r}) Y_{20}(\theta, \phi)\, r^2 d\tau \tag{5}$$

The electric quadrupole interaction (E2) is given by:

$$H(E2) = -\frac{e^2}{2}\sqrt{\frac{4\pi}{5}} Q_0 f(r) Y_{20}(\theta, \phi) \tag{6}$$

$f(r) \rightarrow r^{-3}$ when far away from nucleus

$f(r) \rightarrow$ dependent on the exact form of $\rho(\overrightarrow{r})$ when close to the nucleus

Theory

- Energy displacement due to the electric quadrupole interaction:

$$\Delta E_F\,(E2) = 6\frac{K(K+1) - 4/3\,I(I+1)J(J+1)}{4I(2I-1)J(2J-1)}A_2 \tag{7}$$

where $K = F(F+1) - I(I+1) - J(J+1)$.

$$A_2^0 = \frac{2J-1}{2J+2}\,e^2\,Q_0\left\langle\frac{1}{r^3}\right\rangle_{n,J} \tag{8}$$

- Energy displacement due to the magnetic dipole interaction:

$$\Delta E_F(M1) = \frac{1}{2IJ}\left\{F(F+1) - I(I+1) - J(J+1)\right\}A_1 \tag{9}$$

where $A_1 = IJ\alpha$, α.
Binding energy $E_B \propto m_\mu$. Thus, M1 is two orders of magnitude smaller than that of ordinary atoms

$$A_1^0 = \mu_\mu\,g_I\,\mu_N\,\frac{I(I+1)}{J(J+1)}\left\langle\frac{1}{r^3}\right\rangle_{n,J} \tag{10}$$

Lineshape fit

265.832 keV

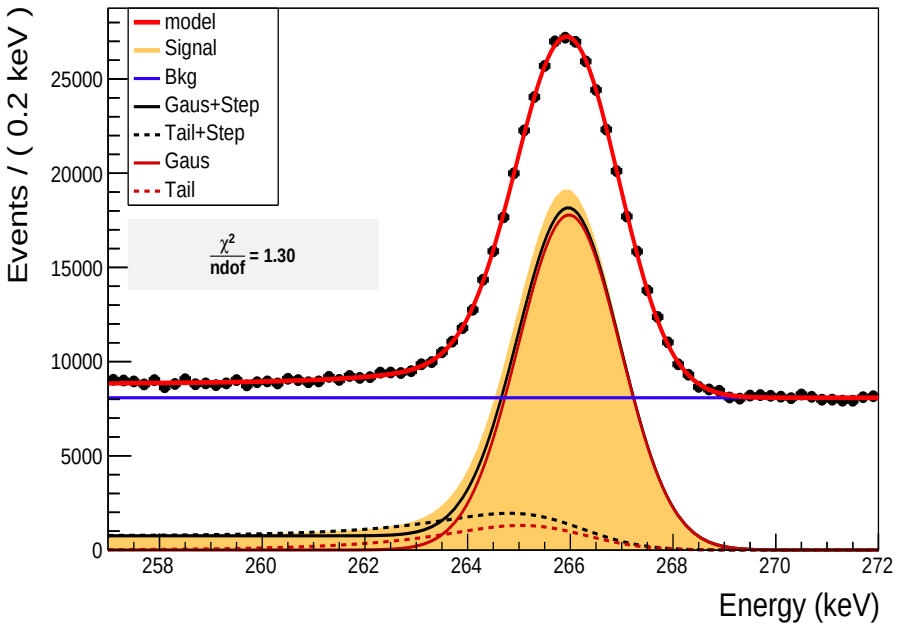

578.56 keV

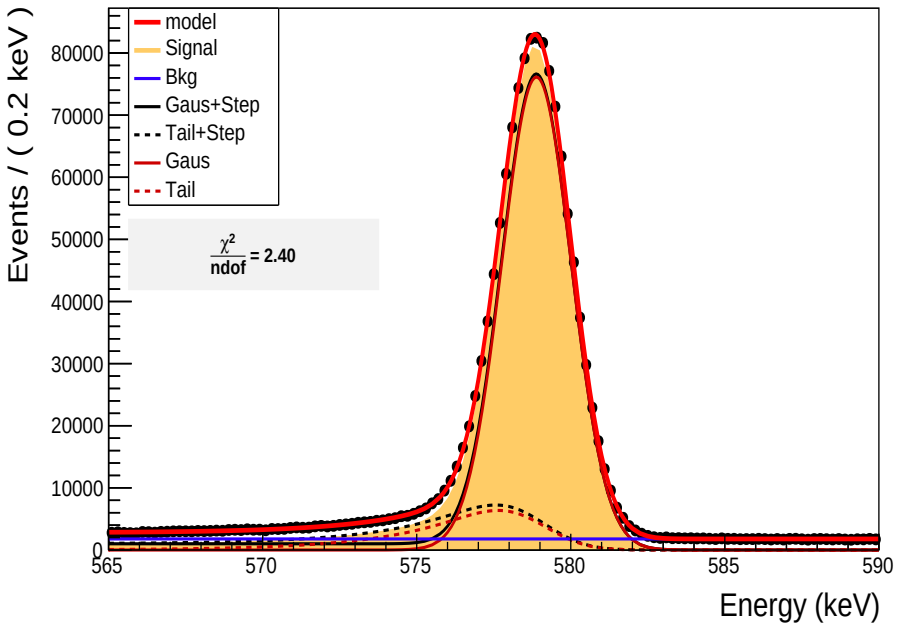

Origin of gamma lines used for the analysis of the line-shape

E (keV)	Origin	Dataset time cut (ns)
265.832	γ-line in $^{206}\mathrm{Tl}$ $\mu^- + {}^{208}\mathrm{Pb} \rightarrow {}^{208}\mathrm{Tl} + \nu_\mu \rightarrow {}^{206}\mathrm{Tl} + 2n$	$^{208}\mathrm{Pb}$ < 700
578.56	2p-1s in $\mu^{35}\mathrm{Cl}$	$^{185}\mathrm{Re}$, $^{187}\mathrm{Re}$ < 300

Fit of the 351.932 keV peak

Origin: decay chain of $^{238}\mathrm{U}$ ($^{214}\mathrm{Pb}$)
$^{214}\mathrm{Pb}$(26.8 min) β-decay
$^{214}\mathrm{Bi}$ γ-line

Energy resolution in Germanium detector

Overall energy resolution in Ge detector is determined by a combination of three factors as:

$$W_T^2 = W_D^2 + W_X^2 + W_E^2 \tag{11}$$

- W_D: statistical fluctuation in the number of charge carriers created
- W_X: due to incomplete charge collection (more significant at detectors of large volume and low average electric field)
- W_E: accounts for the broadening effects due to electronic noise

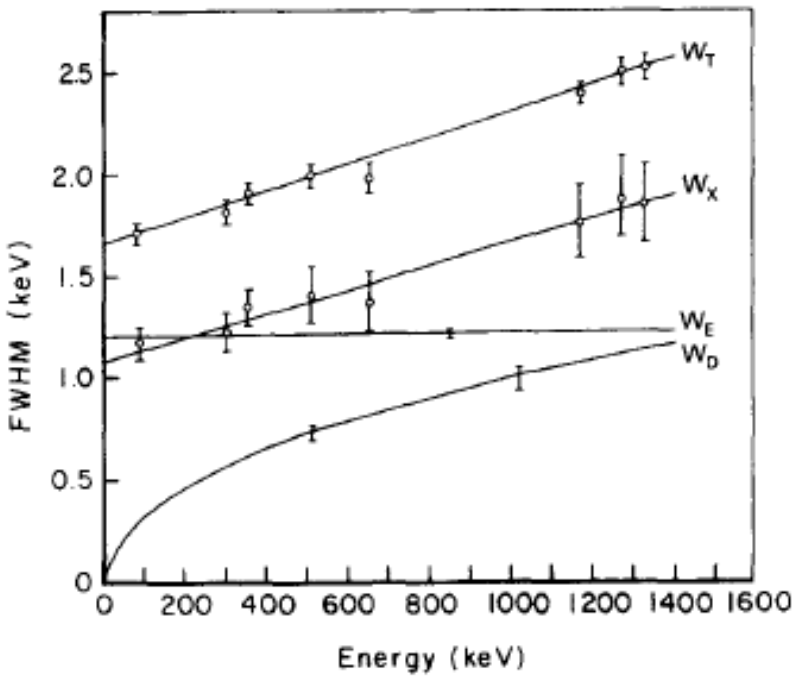

FWHM variation with gamma-ray energy of an 86 cm^3 HPGe detector

Natural line-width

- Natural width of the line $\sim$ quantum mechanical uncertainty in the energy E of levels with finite lifetimes

  If an energy level above ground state has energy E and lifetime Δt, it has energy uncertainty: $\Delta E \Delta t \sim \hbar$ (faster the transition, larger the width). Then, the photon emitted in a transition from this level to the ground level has a range of possible frequencies:

$$\Delta\nu \sim \frac{\Delta E}{h} \sim \frac{1}{2\pi\Delta t}$$

- The FWHM of measured X-ray peak Γ_m is related to the natural (lorentzian) width Γ_n and the instrumental resolution Γ_i (assumed to be Gaussian) by,

$$\Gamma_n = \Gamma_m - \Gamma_i^2/\Gamma_m$$

Peak under 5g-4f hf region

365.5 keV (14.59 μs): γ-line in ^{181}W

$$\mu^- + {}^{185}\mathrm{Re} \rightarrow {}^{185}\mathrm{W}^* + \nu_\mu \rightarrow {}^{181}\mathrm{W} + 4n$$

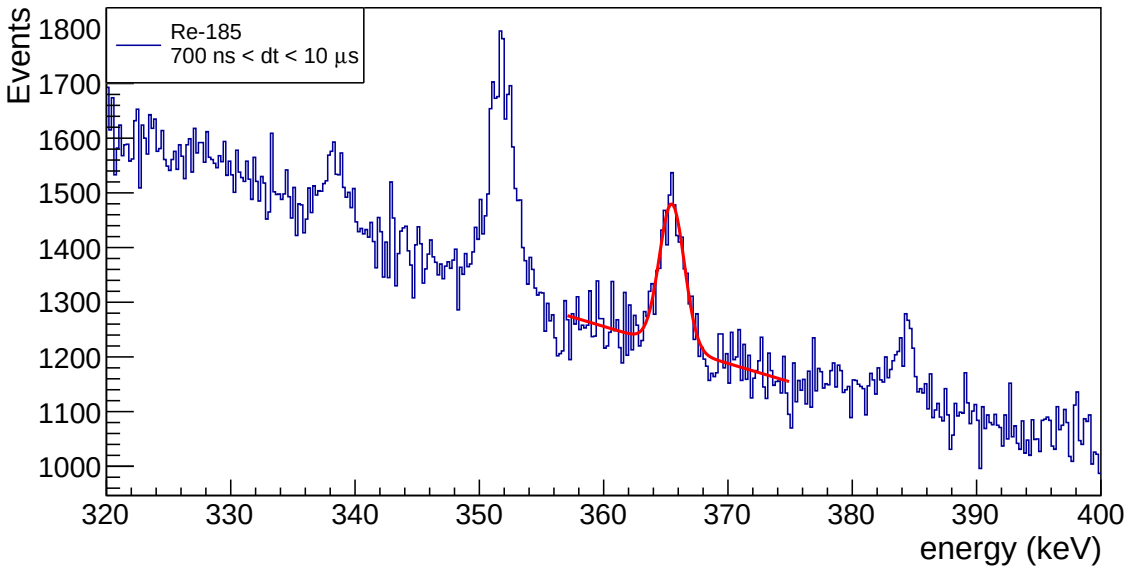

NO.	NAME	VALUE	ERROR
1	p0 counts	6.58095e+02	4.46067e+01
2	p1 mean	3.65489e+02	6.75885e-02
3	p2 sigma	1.00341e+00	6.99741e-02
4	p3	3.69186e+03	2.61751e+02
5	p4	-6.76684e+00	7.14220e-01